frontiers | Frontiers in Pharmacology

ORIGINAL RESEARCH
published: 12 May 2022
doi: 10.3389/fphar.2022.895556

Application of Physiologically Based Pharmacokinetic Modeling in Preclinical Studies: A Feasible Strategy to Practice the Principles of 3Rs

Yawen Yuan[1,2†], Qingfeng He[1†], Shunguo Zhang[2], Min Li[1], Zhijia Tang[1], Xiao Zhu[1], Zheng Jiao[3], Weimin Cai[1] and Xiaoqiang Xiang[1]**

[1]Department of Clinical Pharmacy and Pharmacy Administration, School of Pharmacy, Fudan University, Shanghai, China, [2]Department of Pharmacy, Shanghai Children's Medical Center, School of Medicine, Shanghai Jiao Tong University, Shanghai, China, [3]Department of Pharmacy, Shanghai Chest Hospital, Shanghai Jiao Tong University, Shanghai, China

OPEN ACCESS

Edited by:
Shuiying Hu,
The Ohio State University,
United States

Reviewed by:
Yang Lu,
China Pharmaceutical University,
China
Yizhen Guo,
The Ohio State University,
United States

***Correspondence:**
Weimin Cai
weimincai@fudan.edu.cn
Xiaoqiang Xiang
xiangxq@fudan.edu.cn

[†]These authors have contributed equally to this work

Specialty section:
This article was submitted to Drug Metabolism and Transport, a section of the journal Frontiers in Pharmacology

Received: 14 March 2022
Accepted: 14 April 2022
Published: 12 May 2022

Citation:
Yuan Y, He Q, Zhang S, Li M, Tang Z, Zhu X, Jiao Z, Cai W and Xiang X (2022) Application of Physiologically Based Pharmacokinetic Modeling in Preclinical Studies: A Feasible Strategy to Practice the Principles of 3Rs. Front. Pharmacol. 13:895556. doi: 10.3389/fphar.2022.895556

Pharmacokinetic characterization plays a vital role in drug discovery and development. Although involving numerous laboratory animals with error-prone, labor-intensive, and time-consuming procedures, pharmacokinetic profiling is still irreplaceable in preclinical studies. With physiologically based pharmacokinetic (PBPK) modeling, the *in vivo* profiles of drug absorption, distribution, metabolism, and excretion can be predicted. To evaluate the application of such an approach in preclinical investigations, the plasma pharmacokinetic profiles of seven commonly used probe substrates of microsomal enzymes, including phenacetin, tolbutamide, omeprazole, metoprolol, chlorzoxazone, nifedipine, and baicalein, were predicted in rats using bottom-up PBPK models built with *in vitro* data alone. The prediction's reliability was assessed by comparison with *in vivo* pharmacokinetic data reported in the literature. The overall predicted accuracy of PBPK models was good with most fold errors within 2, and the coefficient of determination (R^2) between the predicted concentration data and the observed ones was more than 0.8. Moreover, most of the observation dots were within the prediction span of the sensitivity analysis. We conclude that PBPK modeling with acceptable accuracy may be incorporated into preclinical studies to refine *in vivo* investigations, and PBPK modeling is a feasible strategy to practice the principles of 3Rs.

Keywords: physiologically based pharmacokinetic modeling, 3Rs, preclinical studies, alternative for animal experiments, bottom-up model

1 INTRODUCTION

The pharmacokinetics study, including examining absorption, distribution, metabolism, and excretion (ADME) profiles of therapeutic agents, plays a vital role in drug discovery and development (Prentis et al., 1988). Because of poor extrapolation from *in vitro* to *in vivo* efficacy, pharmacokinetics profiling processes are routinely implemented in the pharmaceutical industry for early preclinical optimization (Lin and Lu, 1997). However, such processes commonly involve error-prone, labor-intensive, and time-consuming procedures. Not to mention ethics and the welfare of laboratory animals. It was estimated that more than 100 million laboratory animals were

sacrificed for biomedical research annually (Taylor and Alvarez, 2019). Therefore, William Russel and Rex Burch proposed the 3Rs principle (replacement, reduction, and refinement) in 1959 (Vitale et al., 2009; Wachsmuth et al., 2021), attempting to reduce animal use. The 2010 EU Directive states that animals have intrinsic values that need to be respected and that animal experiments should be carefully evaluated in biomedical research, with animal welfare considerations a top priority. Currently, the 3Rs have evolved into basic requirements for researchers to comply with based on animal welfare legislation. Several non-animal testings, including *in vitro* and *in silico* approaches describing the ADME properties, have also been developed to achieve high-throughput screening in drug development. However, unlike understanding the all-inclusive fate of compounds in the body through animal experiments, these conventional *in vitro* methods generally only cover a single-ADME process (Pelkonen and Turpeinen, 2007; Cascone et al., 2016). For example, the commonly used *in vitro* methods for studying drug absorption (Irvine et al., 1999; Verhoeckx et al., 2015; Dargó et al., 2019) or metabolism (Raunio et al., 2004; Hariparsad et al., 2006; Pelkonen and Turpeinen, 2007; van de Kerkhof et al., 2007), such as artificial biofilm models, cell models, and microsomal experiments. Similarly, *in silico* approaches, including the quantitative structure–activity relationship construction model (QSAR), were generally applied to predict the individual biological activity of candidate compounds such as apparent permeability (P_{app}), plasma protein binding rate, and apparent volume of distribution (Vd_{ss}) in the early drug discovery process (Ekins et al., 2000; Yamashita and Hashida, 2004; Lombardo et al., 2017). Despite the abundant data sources, a key challenge remains in correlating the *in vitro* results of ADME features to establish *in vivo* models to reflect the overall disposal.

PBPK modeling was raised back in 1937 and initially applied in predicting the distribution of environmental compounds in mammalian tissues (Lindstrom et al., 1974), and further gradually used for drug exposure prediction, dose extrapolation, and safety assessment (Andersen et al., 1987; Haddad et al., 2001; Meek et al., 2013; Li et al., 2021). PBPK modeling is a mathematical method following the material balance principle to predict the time course of xenobiotic levels in plasma and tissues based on the physiochemical and pharmacokinetic parameters of compounds (Nestorov, 2003). Tremendous progress has been made in PBPK modeling during the past decade. In addition to the rapidly gained industrial recognition (Rowland et al., 2011; Miller et al., 2019), PBPK analysis has also become a routine for the regulatory authorities, especially the United States Food and Drug Administration (FDA), upon new drug applications since 2016 (Zhang et al., 2020).

Currently, the PBPK model has been widely used in various stages of drug development (Chen et al., 2012; Huang et al., 2013), such as evaluating interspecies differences, drug–drug interactions (Jin et al., 2022), targeted tissue exposure, and disease effect (Rostami-Hodjegan and Tucker, 2007; Clewell and Clewell, 2008; Hans and Ursula, 2009; Rietjens et al., 2010; Mielke et al., 2011; Ball et al., 2014). In addition to the top–down modeling, many PBPK models have adopted *in vitro* PK parameters for bottom–up modeling or experimental *in vivo* parameters for "middle-out" approaches as preliminary verification and model optimization (Rostami-Hodjegan and Tucker, 2007; Rietjens et al., 2010; Kostewicz et al., 2014; Templeton et al., 2018; Chang et al., 2019; Umehara et al., 2019). Moreover, given some mechanistic reasons (such as paracellular absorption, active absorption, and targeted transport), many bottom–up PBPK models still require animal data (Wagner, 1981; Clewell and Clewell, 2008). For example, the distribution parameters used in many PBPK models are tissue partition coefficients or steady state distribution parameters from *in vivo* experiments (Harrison and Gibaldi, 1977; Igari et al., 1983; S et al., 2007; T'jollyn et al., 2018). A few PBPK modelings are wholly constructed from *in vitro* parameters without *in vivo* parameters to be fitted and optimized, lacking universal application (Cheng and Ng, 2017). Therefore, constructing a universal PBPK model entirely only with *in vitro* data and the issue of estimating the predicted accuracy in the absence of *in vivo* PK data have caused widespread concern recently (Ellison, 2018; Paini et al., 2019).

To evaluate the feasibility of using PBPK modeling as an alternative for animal experiments, we developed bottom–up PBPK models solely with *in vitro* data using Simcyp® (Sheffield, United Kingdom) to predict the systemic disposition of seven commonly used liver microsomal enzyme probe substrates in rats. The reliability of each prediction was examined with sensitivity analysis. As a practice of 3Rs, this proof-of-concept study will shed light on the refinement of current drug development procedures and may reduce animal usage in drug development.

2 MATERIALS AND METHODS

2.1 Model Inputs Collection

Typical probe substrates of cytochrome P450 (CYP) 1A2, CYP2C9, CYP2C19, CYP2D6, CYP2E1, CYP3A4/5, and UDP-glucuronosyltransferase (UGT), namely, phenacetin, tolbutamide, omeprazole, metoprolol, chlorzoxazone, nifedipine, and baicalein were used as model drugs. The *in vitro* parameters were divided into three categories. Physical chemistry and blood binding-related parameters include molecular weight (MW), neutral species octanol: water partition coefficient ($\log P_{o:w}$), compound type (base/acid/mono/diprotic/ampholyte), negative decadic logarithm of the ionization constant of an acid (pK_a), blood to plasma partition ratio (B/P), and fraction unbound in plasma (f_u). Distribution is affected by the free fraction and the lipid solubility of the drug, which is related to the physiological characteristics mentioned, such as $\log P_{o:w}$, pK_a, and $f_{u.}$ Parameters about absorption include apparent permeability coefficients (P_{app}), polar surface area (PSA), and hydrogen bond donors (HBD). *In vivo* elimination can be extrapolated *via* a well-stirred liver model together with the parallel tube model (Pang and Rowland, 1977) and the dispersion model (Iwatsubo et al., 1997) using *in vitro* metabolic data, including Michaelis–Menten constant for metabolism (K_m), maximum velocity for metabolism (V_{max}),

TABLE 1 | *In vitro* parameters used in each module of the PBPK model.

Application module	*In vitro* parameter	Unit	Acquisition method
Physical chemistry and blood binding	MW	g/mol	Calculation
	$\log P_{o:w}$	—	*In vitro* measurement
	Compound type	Base/acid/mono/diprotic/ampholyte	Physicocheistry property
	pK_a	—	*In vitro* measurement[a]
	B/P	—	*In vitro measurement*
	f_u	—	*In vitro* measurement
Absorption	P_{app}	10^{-6} cm/s	*In vitro* experimentation[b]
	PSA	$Å^2$	Calculation or prediction
	HBD	—	Calculation or prediction
Elimination	CL_{int} (liver)	μl/min/mg protein	*In vitro* experimentation[c]
	CL_{int} (liver)	μl/min/10^6 cells	*In vitro* experimentation[d]
	V_{max}, K_m, and fu_{inc} (liver)	pmol/min/mg protein, μM	*In vitro* experimentation[c]
	V_{max}, K_m, and $f_{u,inc}$ (liver)	pmol/min/10^6 cells, μM	*In vitro* experimentation[d]
	CL_{int} (intestine)	μl/min/mg protein	*In vitro* experimentation[e]
	CL_{int} (intestine)	μl/min/g intestine	*In vitro* experimentation[f]
	V_{max}, K_m, and $f_{u,inc}$ (intestine)	pmol/min/mg protein, μM	*In vitro* experimentation[e]
	V_{max}, K_m, and $f_{u,inc}$ (intestine)	pmol/min/g intestine, μM	*In vitro* experimentation[f]

In vitro *measurement of*

[a]*Ionization equilibrium constant.*

[b]*Include Caco-2 cell permeability experiment, MDCK II cell permeability experiment, and PAMPA (parallel artificial membrane permeability assay) experiment.*

[c]*Liver microsome or liver S9 fraction (a post mitochondrial supernatant model containing both the microsomal enzymes and cytosolic fractions of the cell).*

[d]*Hepatocyte experimentation.*

[e]*Intestinal microsome or intestinal S9 fraction.*

[f]*Intestinal slice.*

and intrinsic clearance (CL_{int}). Various *in vitro* data of model drugs collected from different literature and databases (DrugBank, PubChem, HSDB, TOXNET, *etc.*) were compiled in **Supplementary Table S1**, and the units of each parameter were uniformly converted.

2.2 Physiologically Based Pharmacokinetic Modeling

PBPK models were constructed with *in vitro* data alone using Simcyp® (Simcyp Rat Version 16, Certara, Sheffield, United Kingdom). The *in vitro* parameters used in the PBPK model are described in **Table 1**. The first-order one-compartment model was selected, and the gut was considered as a single compartment in this model. The permeability-limited basolateral membrane is assumed to mediate the absorption of drugs from enterocyte to the intestinal interstitial fluid, and effective permeability in rat (P_{eff}) was calculated based on its relationship with P_{eff} in human (Cao et al., 2006), which can be extrapolated from P_{app}, obtained from *in vitro* experiments (Sun et al., 2002; Tchaparian et al., 2008) or predicted using the PSA and HBD models (Winiwarter et al., 1998). Initially, our absorption model adopted the PSA and HBD models. A minimal PBPK model was selected to predict the volume of distribution at steady state (V_{ss}) with *in vitro* parameters of $\log P_{o:w}$, compound type, and pK_a using mechanistic model 2 (Poulin and Theil, 2002; Berezhkovskiy, 2004; Rodgers et al., 2005; Rodgers and Rowland, 2007), which is a preset model in Simcyp. The tissue distribution was predicted using K_p scalar (tissue: plasma partition coefficient) based on a perfusion-limited model. The K_p scalar was selected as 1 by default in our model. The whole organ metabolic clearance pane was selected in the elimination screen. The liver or intestinal clearance was extrapolated *via in vitro* metabolic data.

The drug plasma concentration–time profile and PK parameters {areas under the concentration–time curve to last time point [$AUC_{(0-t)}$], peak plasma concentration (C_{max}), and time to reach C_{max} (T_{max})} after orally administered single-dose of model drugs were predicted. Meanwhile, the PK process of some model drugs administrated with various doses was simulated.

2.2.1 Physiologically Based Pharmacokinetic Model for Phenacetin

The *in vitro* properties of phenacetin collected from various literatures and databases are listed in **Supplementary Table S1**. The reported f_u values ranged from 0.145 to 0.5. The metabolism of phenacetin by CYP1A2 is biphasic in microsome experiments (Kahn et al., 1987). Since the hepatic CL_{int} collected from reported microsome experiments varied widely (0.086–100 μl/min/mg protein), we selected the median value of f_u (0.3225) and hepatic CL_{int} (27 μl/min/10^6 cells, 20.7–78 μl/min/10^6 cells) from hepatocyte experiments as input values in our model. The *in vitro* data parameterized in phenacetin PBPK model are tabulated in **Table 2**. The simulated results of phenacetin after oral administration of 20, 10, and 5 mg/kg in rats were evaluated.

2.2.2 Physiologically Based Pharmacokinetic Model for Tolbutamide

Tolbutamide is mainly eliminated by CYP2C9 in human liver, and by CYP2C6 and CYP2C11 in rats to produce hydroxyl tolbutamide. f_u of tolbutamide varied from 0.0201 to 0.268 (listed in **Supplementary Table S1**), with the calculated

TABLE 2 | Input parameters in the PBPK models.

Parameter/Compound	Phenacetin	Tolbutamide	Omeprazole	Metoprolol	Chlorzoxazone	Nifedipine	Baicalein
MW (g/mol)	179.2	270.35	345.42	267.4	169.56	346.3	270.24
log$P_{o:w}$	1.58	2.34	2.23	2.06	1.6	2.2	1.7
Compound type	Neutral	Monoprotic acid	Ampholyte	Monoprotic base	Monoprotic acid	Monoprotic base	Monoprotic acid
pK_a1	/	5.16	8.8	9.7	8.3	2.82	5.4
pK_a2	/	/	4.2	/	/	/	/
B/P	1	1.33	0.66	1	1.22	0.59	1.27
f_u	0.32	0.048	0.19	0.86	0.27	0.038	0.054
PSA (Å^2)	38.33	80.65	86.7	50.7	38.3	110	87
HBD	1	2	1	2	1	1	3
CL_{int} (LM) (μl/min/mg protein)	27 (μl/min/10^6 cells)	4.7	158	32	14.9	139	436
CL_{int} (IM) (μl/min/mg protein)	/	/	/	10.5	/	6.4	298
V_{max} (IM) (pmol/min/mg)	0.25	/	780	/	/	/	/
K_m (IM) (μM)	56.7	/	6.97	/	/	/	/
$f_{u\ inc}$ (IM)	1	/	1	/	/	/	/

"/" means no input value exists.

median value to be 0.048. The CL_{int} ranged between 2.72 and 8.10 μl/min/mg protein from various literatures and the median of 4.7 μl/min/mg protein was applied in the PBPK model. The same process was performed for other parameters in **Table 2**. The PK parameters of tolbutamide at 50 mg/kg in rats were predicted.

2.2.3 Physiologically Based Pharmacokinetic Model for Omeprazole

As shown in **Supplementary Table S1**, various *in vitro* data were collected and the deviation of the reported *in vitro* parameters from different sources was slight. Omeprazole is rapidly absorbed in rats and the elimination is almost entirely through hepatic and intestinal metabolism *via* CYP2C19 (Regårdh et al., 1985; Paul, 1991). The penetration of omeprazole into the red cells is low with the value of B/P at 0.6~0.8 and the f_u is about 15% in rat plasma. Similarly, the median values of parameters were calculated for model construction (**Table 2**). Plasma concentration over time in rats following oral administration of omeprazole at 10, 20, and 40 mg/kg was predicted, respectively.

2.2.4 Physiologically Based Pharmacokinetic Model for Metoprolol

The elimination of metoprolol *in vivo* is mainly through liver CYP2D6 in human, leading to extensive first-pass effect and low bioavailability. In addition to CYP2D6, CYP3A also participates in the metoprolol metabolism in rats. As shown in **Supplementary Table S1**, f_u ranged from 0.8 to 0.925, the range of CL_{int} [liver microsomes (LM)] was 17.1–59.9 μl/min/mg protein and the range of CL_{int} [intestine microsomes (IM)] was 7.37–14.7 μl/min/mg protein. The median value of varied parameters was calculated as input parameters in **Table 2**. The disposition process of metoprolol in rats after oral administration of 2.5, 5, and 20 mg/kg was predicted.

2.2.5 Physiologically Based Pharmacokinetic Model for Chlorzoxazone

Chlorzoxazone is the probe substrate of CYP2E1. As shown in **Supplementary Table S1**, the value of f_u ranged from 0.046 to 0.373 and the CL_{int} was from 5.00 to 38.8 μl/min/mg protein. The value of other parameters collected from different sources was relatively consistent. Similarly, the median value was taken as the input value in **Table 2**. Since a dose of 50 mg/kg was frequently used in the PK studies of chlorzoxazone in rats, the PK parameters of chlorzoxazone following oral administration of 50 mg/kg were predicted.

2.2.6 Physiologically Based Pharmacokinetic Model for Nifedipine

Nifedipine is mainly metabolized by CYP 3A1/2 in human and CYP 3A4/5 in rats. As shown in **Supplementary Table S1**, the value of f_u was 0.01–0.08, and the median value was calculated for input. The clearance of nifedipine was found related to concentration (Iwao et al., 2002). The CL_{int} in the liver was 159 μl/min/mg protein when the concentration was 1–5 μM, which was reduced to 119 μl/min/mg protein when the concentration ranged from 5 to 100 μM and eventually dropped to 10 μl/min/mg protein with concentration higher than 100 μM. The value of CL_{int} of small intestinal metabolism was estimated at 6.4 μl/min/mg protein when the concentration was lower than 5 μM and reduced to 2.8 μl/min/mg protein as the concentration was increased to 100 μM. Since the concentration in the liver was unlikely to be higher than 100 μM, the median of hepatic CL_{int} was calculated to be 139 μl/min/mg protein with the ignorance of the lowest value at 10 μl/min/mg protein. The median of CL_{int} of small intestinal metabolism was also calculated for the PBPK model (**Table 2**). The PK parameters of nifedipine in rats after oral administration of 3, 5, and 6 mg/kg were predicted.

2.2.7 Physiologically Based Pharmacokinetic Model for Baicalein

Baicalein, a bioactive flavonoid presented in the root of *Scutellaria baicalensis*, is isolated from traditional Chinese medicine "Huang Qin." Baicalein was reported to be subjected to extensive first-pass metabolism due to the conjugated process by UGT in the liver and intestine. Few *in vitro* data were reported (listed in **Supplementary Table S1**), and the median value was calculated for model construction (shown in **Table 2**). The PK parameters of

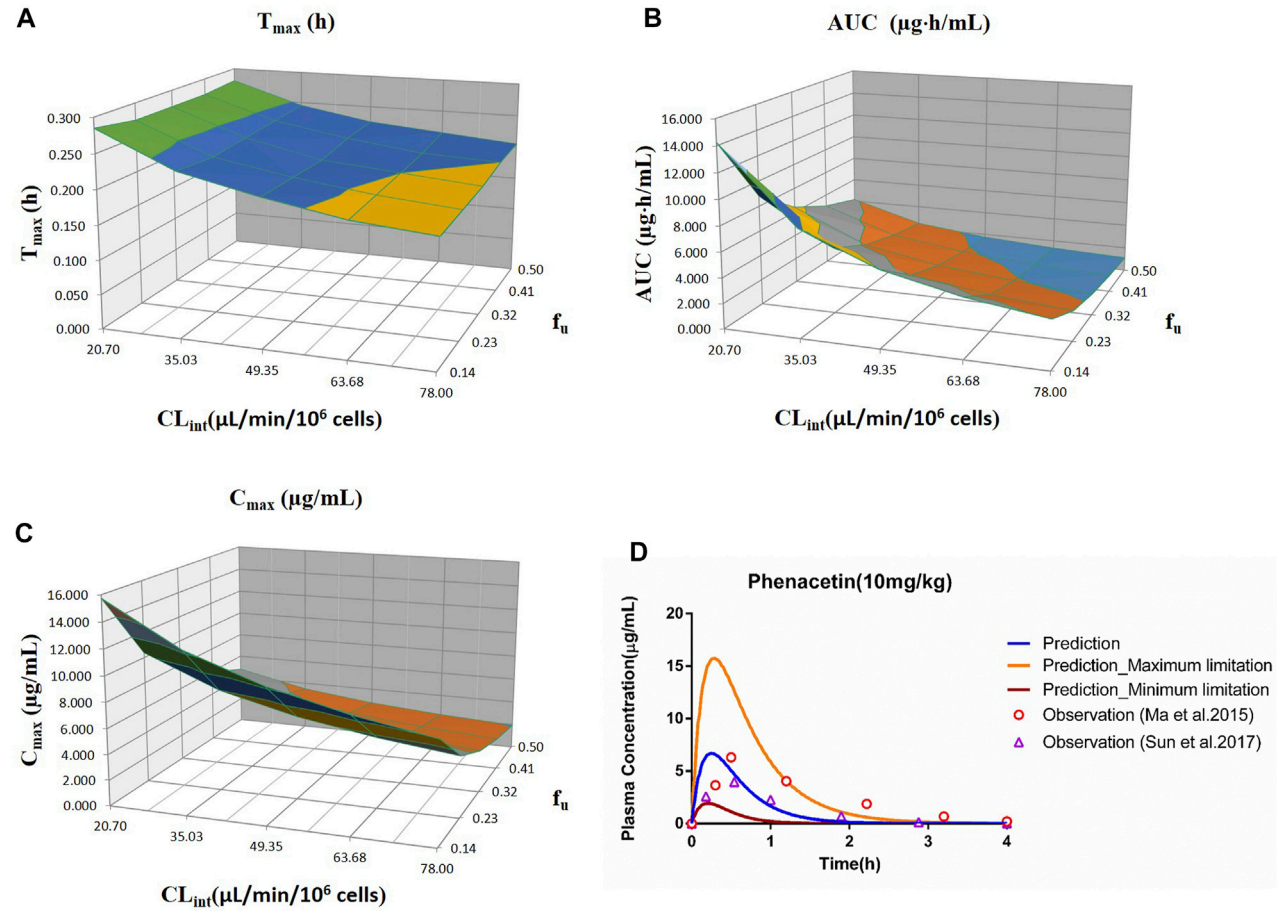

FIGURE 1 | Influence of f_u and CL_{int} (hepatocytes) on the predicted T_{max} **(A)**, $AUC_{(0-t)}$ **(B)**, C_{max} **(C)**, and plasma concentration–time profile **(D)** of the phenacetin PBPK model. Each color in the 3D plots in **(A–C)** represents a prediction range.

baicalein in rats after oral administration of 121 mg/kg were predicted.

2.3 Pharmacokinetic Data

PK parameters ($AUC_{(0-t)}$, C_{max}, and T_{max}) of model drugs in rats orally administrated with a different single-dose of the drugs were assembled from the literature. The $AUC_{(0-t)}$, C_{max}, and T_{max} units were unified as μg·h/ml, μg/ml, and h, respectively. The observed drug plasma concentration–time data were extracted from concentration–time course curves using the GetData software (version 2.24, http://getdata-graph-digitizer.com). Multiple records of PK parameters of model drugs were summarized in **Supplementary Table S2**, showing significant variations on PK parameters, with those of reasonable trend from different doses selected to validate prediction accuracy. For example, it was found that the PK parameters of tolbutamide from the literature varied considerably. Interestingly, the values of C_{max} and $AUC_{(0-t)}$ at high doses were lower than low doses for some records (C_{max}: 91.1–151 μg/ml at 20 mg/kg vs. 40.46 μg/ml at 30 mg/kg, $AUC_{(0-t)}$: 761.7217–1,393 μg·h/ml at 20 mg/kg vs. 183.88 μg·h/ml at 20 mg/kg), and T_{max} also varied greatly (0.89–7.1 h). The relatively consistent PK value at a 50 mg/kg dose was finally selected for the tolbutamide PBPK model accuracy evaluation. Meanwhile, it is difficult to detect baicalein's plasma concentration because of the complicated *in vivo* disposition, poor bioavailability, and extensive metabolism, leading to a considerable variation among the PK parameters. The ones after oral administration of 121 mg/kg were selected due to relatively consistent values (shown in **Supplementary Table S2**). Moreover, it was found to be partly due to the species, age, and gender differences of the rats and formulations. For example, it was reported that the $AUC_{(0-t)}$ and C_{max} of metoprolol were 5–7 times higher and 2 times higher in DA (Dark Agouti) rats and Sprague–Dawley rats, respectively, than those in Wistar rats after oral administration of 5 mg/kg (Belpaire et al., 1990; Komura and Iwaki, 2005; Wang et al., 2014; Ma et al., 2015; Sun et al., 2017). The $AUC_{(0-t)}$ of baicalein was 11.7 times higher after oral administration of baicalein–nicotinamide nano-cocrystals than coarse powder, 7.1 times higher than that of baicalein nanocrystals, and 1.8 times higher than that of baicalein–nicotinamide cocrystals (Pi et al., 2019). As a result, our PBPK model was constructed using male

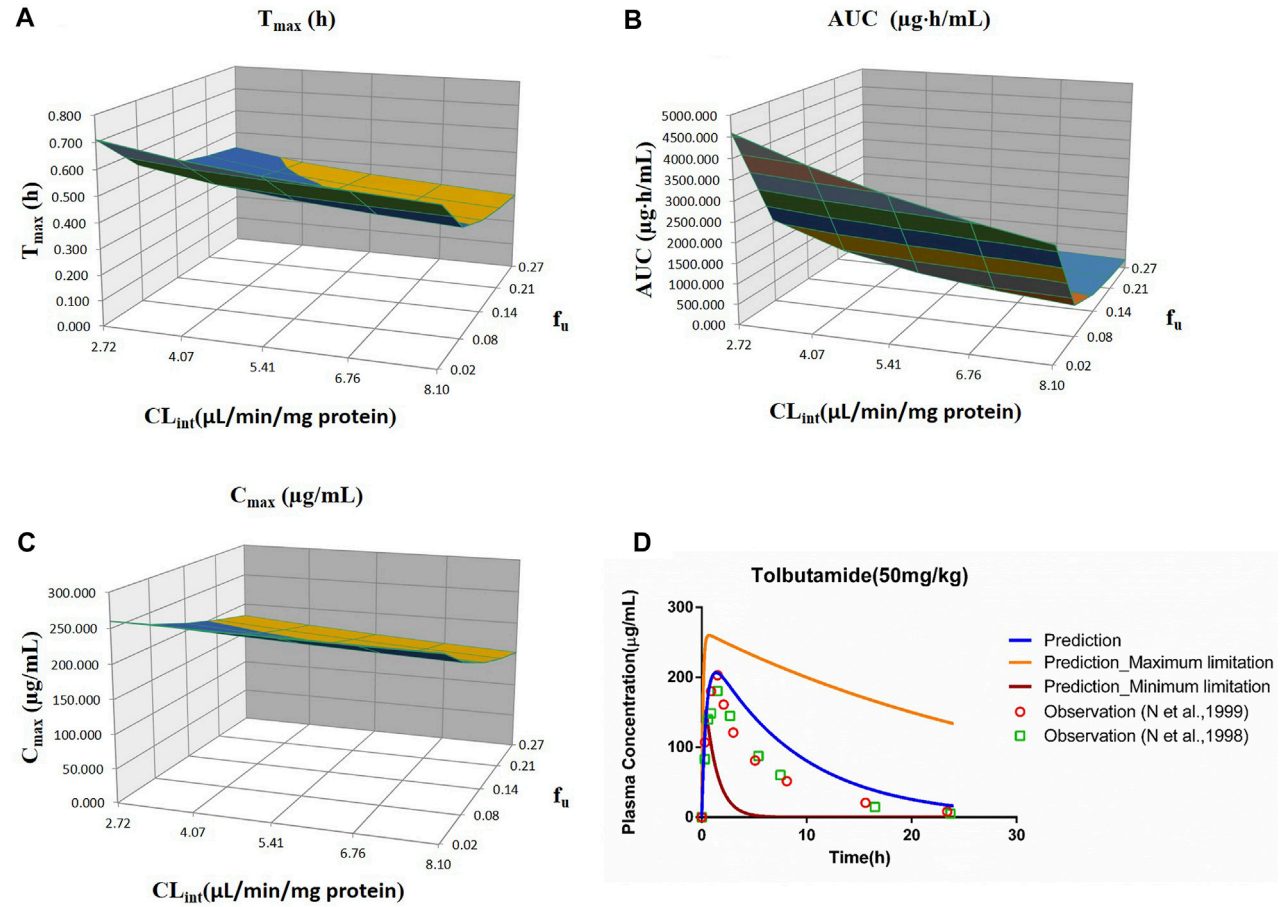

FIGURE 2 | Influence of f_u and CL_{int} (LM) on the predicted T_{max} **(A)**, $AUC_{(0-t)}$ **(B)**, and C_{max} **(C)** and plasma concentration–time profile **(D)** of tolbutamide. Each color in the 3D plots in **(A–C)** represents a prediction range.

Sprague–Dawley rats as the model animal with coarse powder form selected.

2.4 Sensitivity Analysis

As shown in **Supplementary Table S1**, physical chemistry properties such as $\log P_{o:w}$, compound type, pK_a, and B/P and the predicted or calculated properties (MW, PSA, and HBD) were commonly consistent, while the f_u and CL_{int} (LM or hepatocytes) values obtained from the literature varied. To further explore the reliability of the PBPK model, the effect of f_u and CL_{int} (LM or hepatocytes) was investigated. The sensitivity analysis of f_u and CL_{int} (LM or hepatocytes) was determined *via* comparing the predicted results of PBPK models, which were constructed using the range values of f_u and CL_{int} (LM or hepatocytes) with all the other factors maintained constant. The uncertainty range of the PBPK model was defined as the predicted range of the PK parameters in the sensitivity analysis. The sensitivity results were plotted *via* Simcyp and showed in **Figures 1**–**7**. In order to make the 3D plots in A–C in **Figures 1**–**7** more clearly distinguished, the predicted values were divided into 5–8 range values at the same interval, and each range was displayed as a color. Since the colors are numerous and have no special meaning, they are not specifically listed in the figures.

2.5 Model Validation

To verify the prediction accuracy of the PBPK model, we compared the predicted parameters with the experimental data, and fold error was introduced to measure the deviation. The fold error is the ratio between the predicted PK parameters and the corresponding observed values (shown in **Eqs. 1**, **2**). The accuracy of the prediction results increases as the fold error decreases. The simulation is considered acceptable with a fold error of less than 2 (De Buck et al., 2007; Yamazaki et al., 2011).

$$fold\ error = \frac{observed\ parameter}{predicted\ parameter}; if\ observed\ value > predicted\ value \tag{1}$$

$$fold\ error = \frac{predicted\ parameter}{observed\ parameter}; if\ predicted\ value > observed\ value. \tag{2}$$

2.6 Model Performance

R^2, mean absolute error (MAE), and root mean squared error (RMSE) were applied to evaluate the overall performance of the PBPK model. The equations are presented as follows (**Eqs. 3**–**5**). The lower the value of MAE and RMSE and the closer of R^2 to 1, the

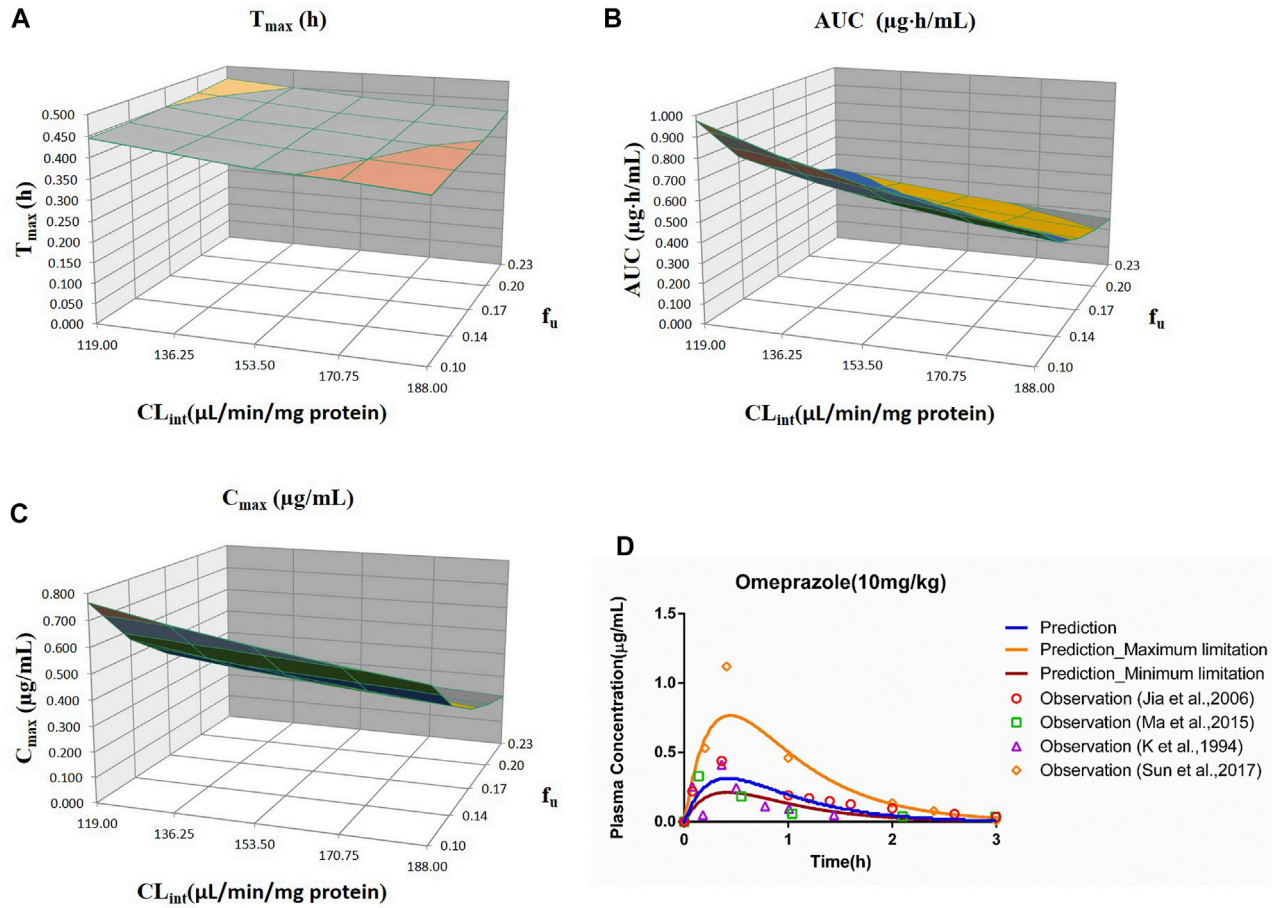

FIGURE 3 | Influence of f_u and CL_{int} (LM) on the predicted T_{max} **(A)**, $AUC_{(0-t)}$ **(B)**, and C_{max} **(C)** and plasma concentration-time profile **(D)** of the omeprazole PBPK model. Each color in the 3D plots in **(A–C)** represents a prediction range.

better the performance of the PBPK model. The performance of the models was plotted using the GraphPad Prism software (version 6).

$$R^2 = 1 - \frac{\sum_i (x_i - y_i)^2}{\sum_i (x_i - \bar{x})^2}, \quad (3)$$

$$MAE = \frac{\sum_1^N |x_i - y_i|}{N}, \quad (4)$$

$$RMSE = \sqrt{\frac{\sum_1^N (x_i - y_i)^2}{N}}. \quad (5)$$

x_i and y_i are the observed and the predicted concentrations, respectively, $\bar{x}$ is the average of the observed values, and $\bar{N}$ is the number of data points.

3 RESULTS

3.1 Physiologically Based Pharmacokinetic Model-Predicted Results

PBPK models for probe drugs (phenacetin, tolbutamide, omeprazole, metoprolol, chlorzoxazone, nifedipine, and baicalein) were constructed using *in vitro* parameters (MW, $\log P_{o:w}$, compound type, pK_a, B/P, f_u, PSA, HBD, CL_{int}, V_{max}, K_m, and $f_{u,inc}$). The predicted results of each drug were presented later, and the PK curves are displayed in **Supplementary Figures S1–S7**.

3.1.1 Phenacetin

The predicted results of the phenacetin PBPK model are shown in **Table 3**. Although the predicted C_{max} was slightly higher than the observed one with the fold error of 1.93 at 5 mg/kg, the fold error values were all within the threshold of 2, indicating good simulation performance. Meanwhile, the predicted data were slightly higher than the observed ones at 5 mg/kg, while other observed points were around the predicted values at 10 and 20 mg/kg (**Supplementary Figure S1**). It could be concluded that the experimental CL_{int} value used in the model was underestimated at 5 mg/kg.

3.1.2 Tolbutamide

The prediction results are listed in **Table 4**. The fold error values were all less than 2 with the observed data around the predicted curve (**Supplementary Figure S2**), suggesting acceptable prediction accuracy.

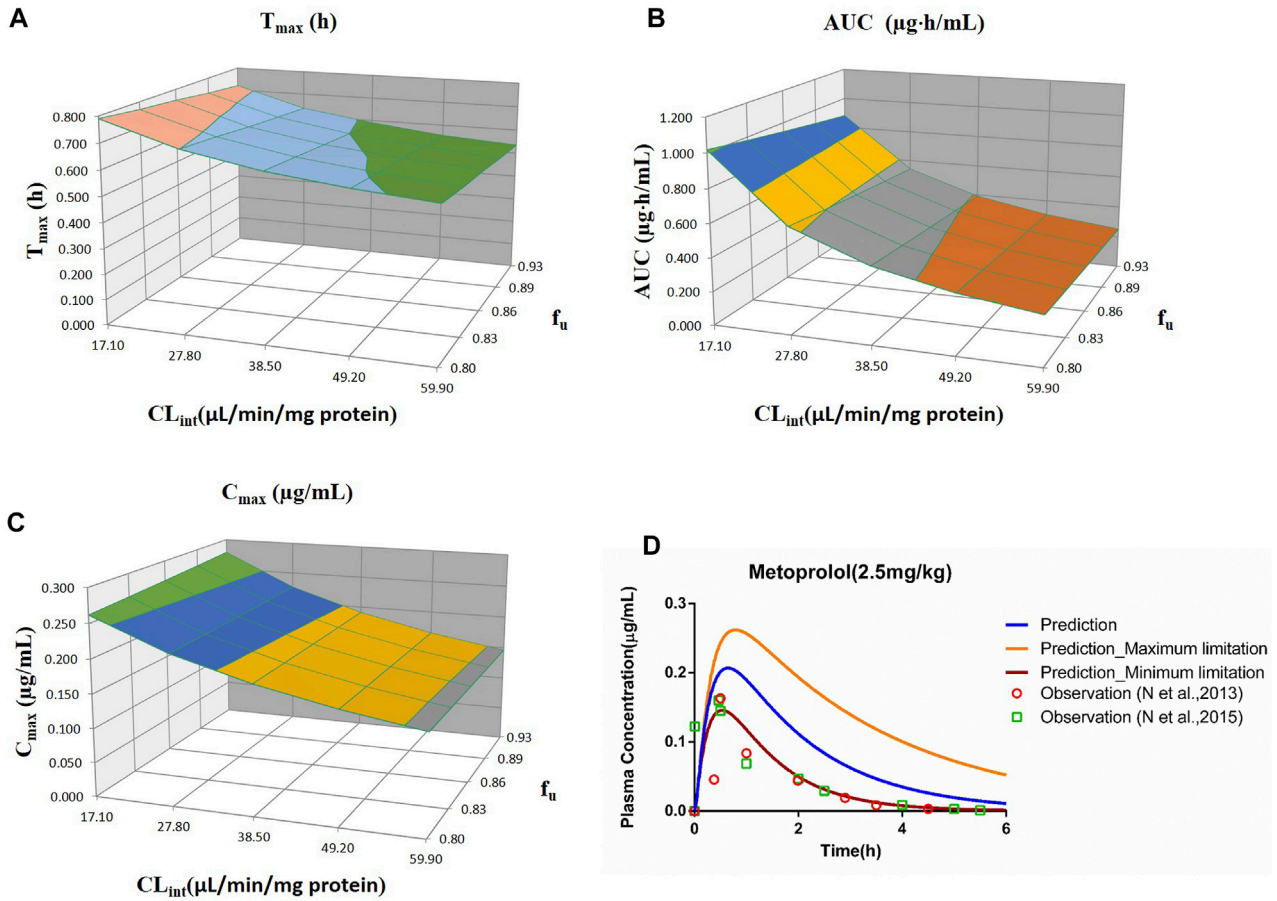

FIGURE 4 | Influence of f_u and CL_{int} (LM) on the predicted T_{max} **(A)**, $AUC_{(0-t)}$ **(B)**, C_{max} **(C)**, and plasma concentration–time profile **(D)** of the metoprolol PBPK model. Each color in the 3D plots in **(A–C)** represents a prediction range.

3.1.3 Omeprazole

The predicted PK parameters of the omeprazole PBPK model were compared with the multiple records of experimental parameters (shown in **Table 5**). Although a few predicted values were slightly lower than the observed ones, most fold errors fell within 2, indicating good predicted accuracy. **Supplementary Figure S3** showed that most of the predicted points were around the observed concentration–time profile.

3.1.4 Metoprolol

The fold errors of the predicted parameters of the metoprolol PBPK model are evaluated in **Table 6**. The values of fold error in the 10 mg/kg group were less than 2, and the trend of the observed data coordinated the predicted profile (**Supplementary Figure S4**), indicating good simulation performance. Overall, all predicted concentration curves were slightly higher than the observation points, which is contributed by underestimating distribution and elimination.

3.1.5 Chlorzoxazone

The predicted results of the chlorzoxazone PBPK model are tabulated in **Table 7**. Most fold errors of predicted parameters were larger than 2. The predicted curve was higher and deviated from the observed data (**Supplementary Figure S5**), which could be related to the underestimation of distribution and elimination. The influence of the two characteristics on the PBPK model will be further explored in the sensitivity analysis.

3.1.6 Nifedipine

The predicted results of the nifedipine PBPK model are shown in **Table 8**. The fold error of C_{max} and $AUC_{(0-t)}$ mainly were within 2, indicating acceptable prediction performance. Although the difference between predicted T_{max} and the observed values was more than 2 times (2.16 times), with a significant individual variation between the measured values of T_{max} (0.08–1.5 h), the fold errors of C_{max} and $AUC_{(0-t)}$ were within 2, indicating good prediction accuracy. As shown in **Supplementary Figure S6**, the predicted concentration curve was slightly shifted due to the difference in T_{max} at 5 mg/kg, while the observed dots were close to the predicted ones at 3 and 6 mg/kg.

3.1.7 Baicalein

The simulation results are shown in **Table 9**. The predicted curve is shown in **Supplementary Figure S7**. Although the predicted

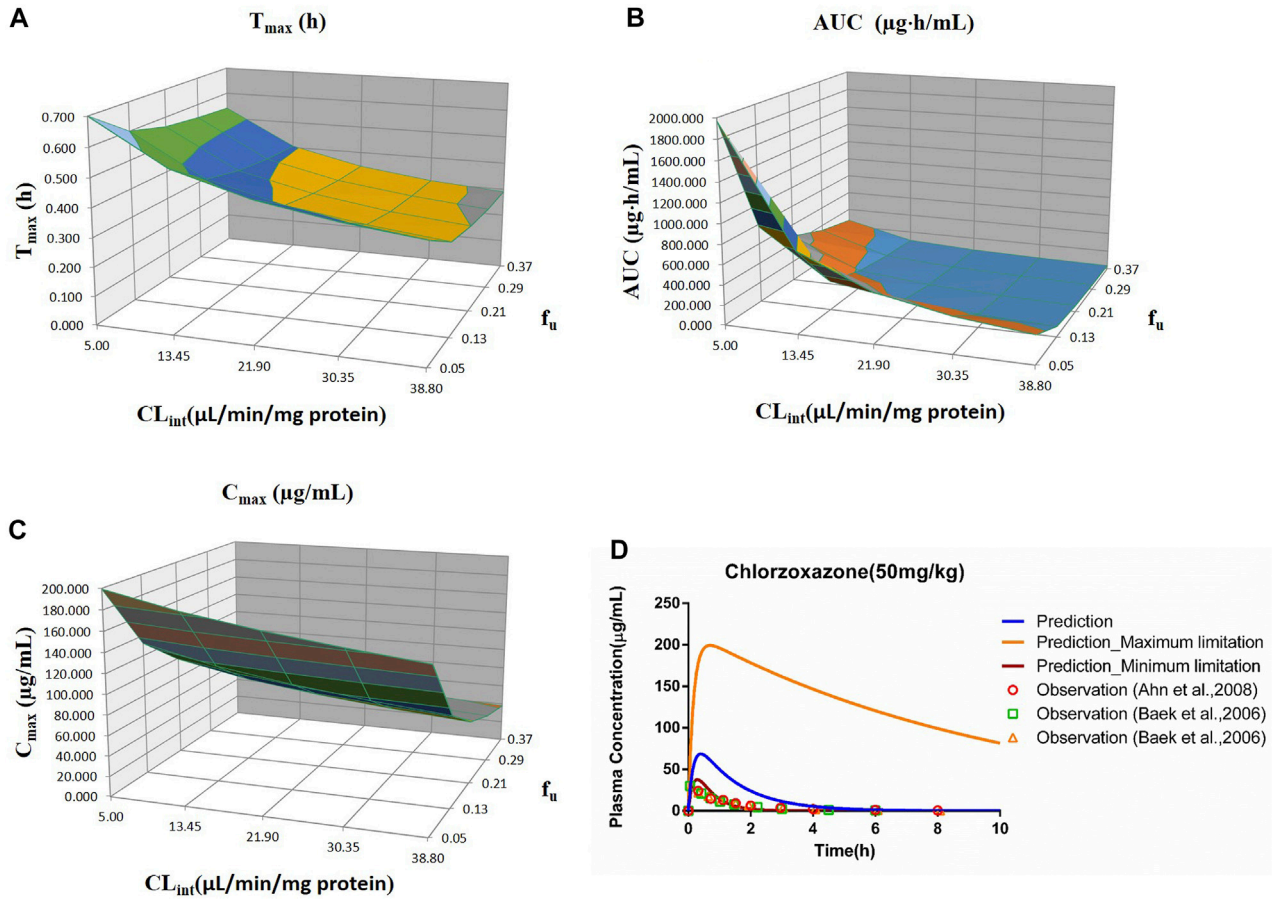

FIGURE 5 | Influence of f_u and CL_{int} (LM) on the predicted T_{max} **(A)**, $AUC_{(0-t)}$ **(B)**, C_{max} **(C)**, and plasma concentration–time profile **(D)** of the chlorzoxazone PBPK model. Each color in the 3D plots in **(A–C)** represents a prediction range.

C_{max} was slightly lower than the observed one, the fold errors were within 2. The observed PK data spread around the predicted profile, suggesting good prediction performance.

3.2 Sensitivity Analysis

The sensitivity analysis of f_u and CL_{int} (LM or hepatocytes) was evaluated with other factors maintained constant. The variation spans of f_u and CL_{int} (LM or hepatocytes) from various literatures are listed in **Table 10**. The uncertainty of the PBPK model-predicted results was estimated based on the range of f_u and CL_{int} (LM or hepatocytes) obtained from various literatures.

3.2.1 Phenacetin

The sensitivity analysis of f_u (0.145–0.5) and CL_{int} (hepatocytes: 20.7–78 μl/min/10^6 cells) for the phenacetin PBPK model was performed at 10 mg/kg (shown in **Figure 1**). The predicted value of T_{max}, C_{max}, and $AUC_{(0-t)}$ ranged from 0.18 to 0.28 h, 1.93 to 15.74 μg/ml, and 1.10 to 14.25 μg·h/ml, respectively. Most concentration points are within the uncertainty range.

3.2.2 Tolbutamide

The sensitivity analysis of f_u (0.0201–0.268) and CL_{int} (LM: 2.72–8.1 μl/min/mg protein) was investigated for the tolbutamide PBPK model at 50 mg/ml (shown in **Figure 2**). As a result, the predicted T_{max}, C_{max}, and $AUC_{(0-t)}$ ranged from 0.32 to 0.71 h, 152.72 to 260.15 μg/ml, and 231.67 to 4,587.60 μg·h/ml, respectively. The observed points were in the area between the median prediction curve and the lowest prediction curve (CL_{int} = 8.1 μl/min/mg protein, f_u = 0.27).

3.2.3 Omeprazole

The range of f_u (0.105–0.232) and CL_{int} (LM: 119–188 μl/min/mg protein) was applied for the sensitivity analysis of the omeprazole PBPK model at 10 mg/kg (shown in **Figure 3**). The results showed that the predicted T_{max}, C_{max}, and $AUC_{(0-t)}$ ranged from 0.38 to 0.46 h, 0.21 to 0.77 μg/ml, and 0.26 to 0.98 μg·h/ml, respectively. As shown in **Figure 3D**, most observation dots were in the sensitivity prediction range.

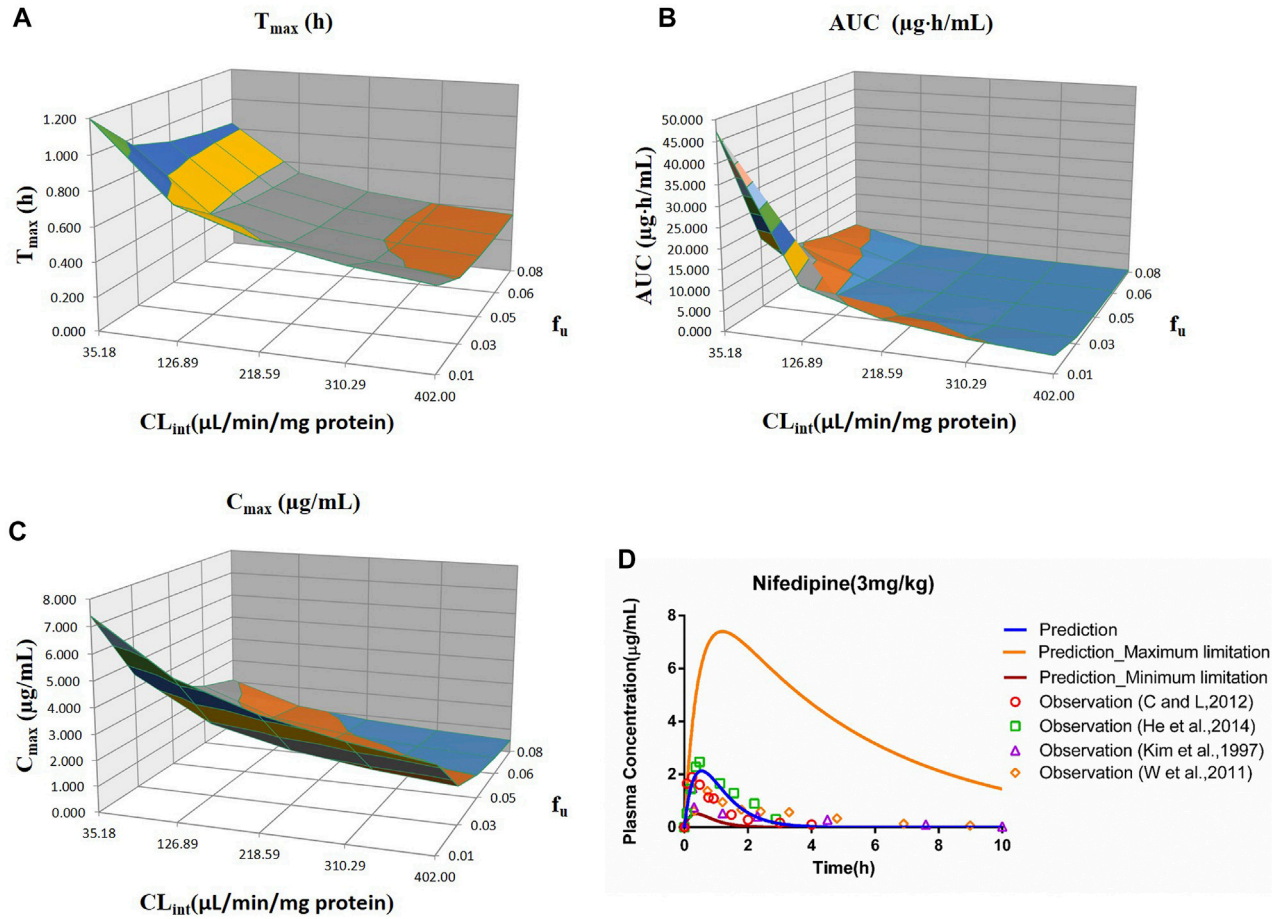

FIGURE 6 | Influence of f_u and CL_{int} (LM) on the predicted T_{max} **(A)**, $AUC_{(0-t)}$ **(B)**, C_{max} **(C)**, and plasma concentration–time profile **(D)** of the nifedipine PBPK model. Each color in the 3D plots in **(A–C)** represents a prediction range.

3.2.4 Metoprolol

The sensitivity analysis of f_u (0.80–0.925) and CL_{int} (LM: 17.1–59.9 μl/min/mg protein) was determined for the metoprolol PBPK model at 2.5 mg/kg in **Figure 4**. The predicted range of T_{max}, C_{max}, and $AUC_{(0-t)}$ were 0.54–0.79 h, 0.15–0.28 μg/ml, and 0.25–1.02 μg·h/ml, respectively. It is illustrated in **Figure 4D** that the observation data were close to the lowest predicted curve.

3.2.5 Chlorzoxazone

Sensitivity analysis of the chlorzoxazone PBPK model was performed at 50 mg/kg with the f_u ranging from 0.046 to 0.373 and CL_{int} (LM) from 5 to 38.8 μl/min/mg protein (shown in **Figure 5**). The results showed the predicted T_{max}, C_{max}, and $AUC_{(0-t)}$ ranged from 0.29 to 0.70 h, 37.69 to 199.27 μg/ml, and 34.69 to 1970.18 μg·h/ml, respectively. The observation dots were around the lowest prediction curve (Prediction_Minimum limitation curve), as shown in **Figure 5D**.

3.2.6 Nifedipine

The sensitivity analysis of f_u (0.01–0.08) and CL_{int} (LM: 35.18–402 μl/min/mg protein) was investigated for the nifedipine PBPK model at 3 mg/kg (shown in **Figure 6**). The predicted T_{max}, C_{max}, and $AUC_{(0-t)}$ ranged from 0.36 to 1.20 h, 0.51 to 7.40 μg/ml, and 0.52 to 47.27 μg·h/ml, respectively. The observation points were centered on the median prediction curve, as shown in **Figure 6D**.

3.2.7 Baicalein

The sensitivity analysis of f_u and CL_{int} (LM) was performed with the range from 0.029 to 0.0791 and 338.9 to 574.11 μl/min/mg protein for the baicalein PBPK model at 121 mg/kg (shown in **Figure 7**). The results showed the predicted T_{max}, C_{max}, and $AUC_{(0-t)}$ ranged from 0.19 to 0.36 h, 0.59 to 2.08 μg/ml, and 0.51 to 2.36 μg·h/ml, respectively. As illustrated in **Figure 7D**, observation dots were within the sensitivity prediction range.

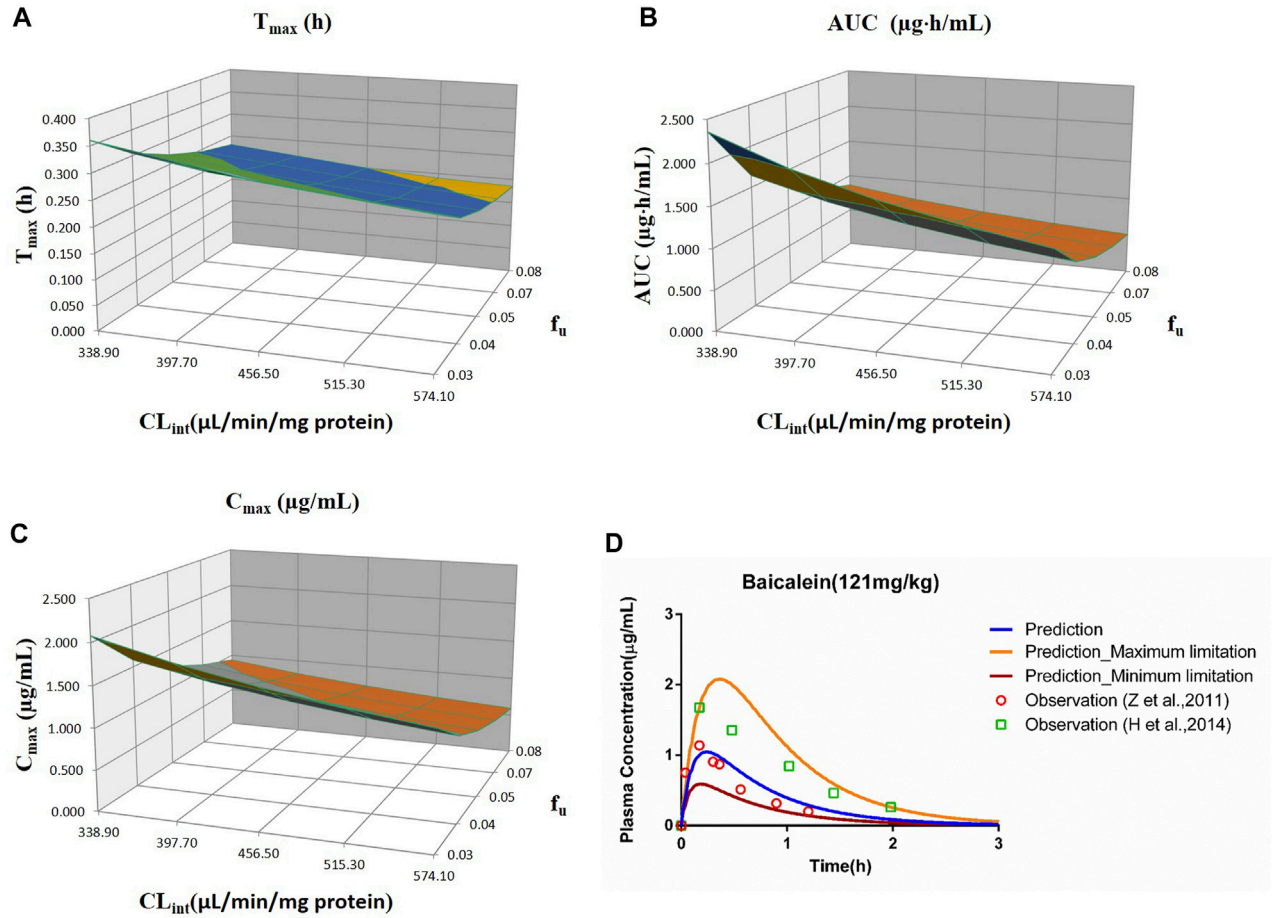

FIGURE 7 | Influence of f_u and CL_{int} (LM) on the predicted T_{max} **(A)**, $AUC_{(0-t)}$ **(B)**, C_{max} **(C)**, and plasma concentration–time profile **(D)** of the baicalein PBPK model. Each color in the 3D plots in **(A–C)** represents a prediction range.

TABLE 3 | Comparison between the predicted and the observed PK parameters of the phenacetin PBPK model.

	Dose	T_{max} (h)	C_{max} (μg/ml)	$AUC_{(0-t)}$ (μg•h/ml)	Reference
5 mg/kg	Prediction	0.25	3.34	2.47	—
	Observation	0.33–0.50	1.73	1.52	Zhou et al. (2014)
	Fold error	1.31–2.00	1.93	1.62	—
10 mg/kg	Prediction	0.25	6.69	4.95	—
	Observation 1	0.50	6.28 ± 1.94	9.79 ± 3.58	Ma et al. (2015)
	Fold error	1.98	1.07	1.98	—
	Observation 2	—	3.94 ± 0.81	4.69 ± 0.86	Sun et al. (2017)
	Fold error	—	1.70	1.06	—
20 mg/kg	Prediction	0.25	13.37	9.90	—
	Observation	0.25	9.00	13.12	Welch et al. (1976)
	Fold error	1.01	1.49	1.33	—

3.3 Physiologically Based Pharmacokinetic Model Performance

The fold errors are summarized in **Figure 8**. Furthermore, to evaluate the overall performance of the PBPK model, we compared the prediction concentration data with the observed ones (n = 390, shown in **Figure 9**). Moreover, the prediction performance of the PBPK model with absorption module using PSA and HBD was compared with that using P_{app} from *in vitro* experiments (Caco-2 experimentation). The input of P_{app} was also applied to the median data of the various values. As shown in **Table 11**, the model performance using PSA and HBD, with a lower value of MAE and RMSE and higher value of R^2, was better

TABLE 4 | Comparison between the predicted PK parameters of the tolbutamide PBPK model and the observed PK parameters at 50 mg/kg.

50 mg/kg p.o.	T_{max} (h)	C_{max} (μg/ml)	$AUC_{(0-t)}$ (μg•h/ml)	Reference
Prediction	1.38	206.74	1965.99	—
Observation 1	0.91 ± 0.37	232.00 ± 35.00	1,309.00 ± 40.00	Nishimura et al. (1999)
Fold error	1.51	1.12	1.50	—
Observation 2	1.42 ± 0.56	176.00 ± 37.20	1,228.00 ± 153.00	Nishimura et al. (1998)
Fold error	1.03	1.17	1.60	—

TABLE 5 | Comparison between the predicted PK parameters of the omeprazole PBPK model and the observed PK parameters.

	Dose	T_{max} (h)	C_{max} (μg/ml)	$AUC_{(0-t)}$ (μg•h/ml)	Reference
10 mg/kg	Prediction	0.42	0.31	0.38	—
	Observation 1	0.36 ± 0.22	0.44 ± 0.12	0.59 ± 0.14	Jia et al. (2006)
	Fold error	1.16	1.40	1.55	—
	Observation 2	0.10 ± 0.10	0.33 ± 0.01	0.47 ± 0.13	Ma et al. (2015)
	Fold error	4.20	1.07	1.24	—
	Observation 3	0.21 ± 0.02	0.50 ± 0.12	0.29 ± 0.07	Kazuhide et al. (1994)
	Fold error	2.00	1.60	1.32	—
	Observation 4		1.13 ± 0.18	1.13 ± 0.16	Sun et al. (2017)
	Fold error		3.60	2.97	—
20 mg/kg	Prediction	0.40	0.81	0.96	—
	Observation 1	0.25 ± 0.02	1.43 ± 0.38	0.86 ± 0.15	Kazuhide et al. (1994)
	Fold error	1.58	1.77	1.11	—
	Observation 2	0.25 ± 0.00	1.01 ± 0.17	0.73 ± 0.06	Watanabe et al. (2002)
	Fold error	1.58	1.25	1.31	—
	Observation 3	0.50 ± 0.00	2.01 ± 0.14	1.50 ± 0.08	Singh and Asad (2010)
	Fold error	1.26	2.49	1.57	—
40 mg/kg	Prediction	0.37	2.88	3.26	—
	Observation 1	0.29 ± 0.22	2.11 ± 0.99	1.57 ± 0.54	Lee et al. (2009)
	Fold error	1.27	1.36	2.08	—
	Observation 2	0.17 ± 0.09	2.61 ± 0.55	2.10 ± 0.93	Young et al. (2007)
	Fold error	2.23	1.10	1.55	—
	Observation 3	0.68 ± 0.82	2.66 ± 2.00	3.08 ± 1.44	Lee et al. (2007b)
	Fold error	1.82	1.08	1.06	—
	Observation 4	0.35 ± 0.39	3.30 ± 1.65	2.27 ± 1.07	Lee et al. (2006)
	Fold error	1.06	1.15	1.44	—
	Observation 5	0.27 ± 0.02	2.44 ± 0.63	2.26 ± 0.52	Kazuhide et al. (1994)
	Fold error	1.38	1.18	1.44	—
	Observation 6	0.10 ± 0.06	4.89 ± 1.33	1.98 ± 0.60	Lee et al. (2007c)
	Fold error	3.58	1.70	1.64	—
	Observation 7	0.35 ± 0.32	2.43 ± 1.17	1.92 ± 0.88	Lee et al. (2007a)
	Fold error	1.05	1.18	1.70	—

than using P_{app} from Caco-2 experimentation. As displayed in **Figure 9B**, prediction 1 was closer to the correlation line with most dots within the ±20% of the observed concentration, indicating the overall good performance of PBPK model construction using the PSA and HBD methods.

4 DISCUSSION

While collecting *in vitro* parameters, we noticed the f_u and CL_{int} from different sources varied; therefore, the median values were applied to construct the model. A sensitivity analysis was performed to further explore the impact of these two parameters on the model prediction accuracy. The overall predicted accuracy of PBPK models using the median value was good with most fold errors within 2, and the R^2 between the predicted concentration data and the observed data was more than 0.8 (**Figures 8**, **9**). However, there was an exception that the chlorzoxazone PBPK model using median data was not satisfying with the prediction results, which is 2 times higher than the observed ones. It could be related to the underestimated distribution and clearance. In terms of the sensitivity analysis, the observed points were closest to the lowest prediction curve with the highest CL_{int} (38.8 μl/min/mg protein) and f_u 0.373 (Moon et al., 2003; Baek et al., 2006). The lowest prediction parameters of T_{max}, C_{max}, and $AUC_{(0-t)}$ were 0.29 h, 37.69 μg/ml, and 34.69 μg·h/ml, respectively. Moreover, most of the fold errors were within 2 (observation 1–3), indicating good prediction accuracy. Similarly, the prediction result of metoprolol using the median PBPK model was also slightly higher at 2.5 mg/kg, and the observed data was close to the lowest predicted curve. The prediction T_{max}, C_{max}, and $AUC_{(0-t)}$ of the metoprolol PBPK model using highest experimental CL_{int} (59.9 μl/min/mg) and f_u (0.93) at 2.5 mg/kg

TABLE 6 | Comparison between the predicted PK parameters of metoprolol PBPK models and the observed PK parameters at different doses.

	Dose	T_{max} (h)	C_{max} (μg/ml)	$AUC_{(0-t)}$ (μg•h/ml)	Reference
2.5 mg/kg	Prediction	0.65	0.21	0.51	—
	Observation 1	0.50 ± 0.00	0.16 ± 0.00	0.21 ± 0.02	Nandi et al. (2013)
	Fold error	1.30	1.27	2.39	—
	Observation 2	0.47 ± 0.07	0.16 ± 0.01	0.22 ± 0.02	Nandi et al. (2015)
	Fold error	1.37	1.29	2.28	—
5 mg/kg	Prediction	0.65	0.41	1.01	—
	Observation	0.50	0.40	0.45	Komura and Iwaki (2005)
	Fold error	1.30	1.04	2.25	—
10 mg/kg	Prediction	0.65	0.83	2.02	—
	Observation 1	0.60 ± 0.30	0.57 ± 0.25	1.66 ± 0.58	Ma et al. (2015)
	Fold error	1.08	1.45	1.22	—
	Observation 2	0.70 ± 0.50	0.81 ± 0.28	1.35 ± 0.59	Wang et al. (2014)
	Fold error	1.08	1.02	1.50	—
	Observation 3	—	0.53 ± 0.066	1.49 ± 0.39	Sun et al. (2017)
	Fold error	—	1.56	1.35	—

TABLE 7 | Comparison between the predicted PK parameters of the chlorzoxazone PBPK model and the observed PK parameters at 50 mg/kg.

50 mg/kg p.o.	T_{max} (h)	C_{max} (μg/ml)	$AUC_{(0-t)}$ (μg•h/ml)	Reference
Prediction	0.40	68.66	124.78	—
Observation 1	0.25 (0.25–0.50)	23.10 ± 8.59	41.67 ± 8.48	Ahn et al. (2008)
Fold error	1.58	2.97	2.99	—
Observation 2	0.14 ± 0.08	31.80 ± 13.10	46.83 ± 16.00	Baek et al. (2006)
Fold error	2.85	2.16	2.66	—
Observation 3	0.10 ± 0.06	30.50 ± 8.17	39.83 ± 4.08	Baek et al. (2006)
Fold error	3.81	2.25	3.13	—

TABLE 8 | Comparison between the predicted PK parameters of nifedipine PBPK models and the observed PK parameters at different doses.

	Dose	T_{max} (h)	C_{max} (μg/ml)	$AUC_{(0-t)}$ (μg•h/ml)	Reference
3 mg/kg	Prediction	0.54	2.13	3.18	—
	Observation 1	0.25 (0.08–0.50)	2.00 ± 0.68	2.23 ± 0.42	Choi and Lee (2012)
	Fold error	2.16	1.07	1.42	—
	Observation 2	0.47 ± 0.03	2.46 ± 0.29	4.30 ± 0.45	He et al. (2014)
	Fold error	1.14	1.15	1.35	—
	Observation 3	0.25	1.48 ± 0.38	2.84 ± 0.19	Kim et al. (1997)
	Fold error	2.16	1.44	1.12	—
	Observation 4	0.58 ± 0.13	1.68 ± 0.58	3.38 ± 0.60	Wang et al. (2011)
	Fold error	1.07	1.27	1.06	—
5 mg/kg	Prediction	0.54	3.56	5.30	—
	Observation 1	0.38 ± 0.06	1.76 ± 0.20	2.72 ± 0.34	Mutsunobu et al. (2004)
	Fold error	1.42	2.02	1.95	—
	Observation 2	0.25 (0.12–0.50)	1.95 ± 0.26	2.73 ± 0.40	Ikehata et al. (2008)
	Fold error	2.16	1.82	1.94	—
	Observation 3	0.25 (0.12–1.50)	1.96 ± 0.23	3.75 ± 0.63	Ikehata et al. (2008)
	Fold error	2.16	1.81	1.41	—
	Observation 4	0.25 (0.12–1.00)	2.56 ± 0.23	4.38 ± 0.29	Ikehata et al. (2008)
	Fold error	2.16	1.39	1.21	—
6 mg/kg	Prediction	0.54	4.27	6.36	—
	Observation 1	0.38 (0.20–0.57)	5.23 (4.55–6.01)	5.75 (4.72–6.98)	Grundy et al. (1998)
	Fold error	1.41	1.23	1.11	—
	Observation 2	0.28 (0.16–0.40)	5.88 (3.33 ± 10.40)	5.90 (4.73–7.35)	Grundy et al. (1997)
	Fold error	1.94	1.38	1.08	—

were 0.53 h, 0.15 μg/ml, and 0.25 μg·h/ml, respectively and the fold errors were within 2 (Belpaire et al., 1989; Yoon et al., 2011). These results suggest that applying the PBPK model using *in vitro* parameters in the early screening of candidate compounds is feasible and helpful, and the prediction accuracy of the model is related to the *in vitro* parameters, especially f_u and CL_{int}. It is worth

TABLE 9 | Comparison between the predicted PK parameters of the baicalein PBPK model and the observed PK parameters at 121 mg/kg.

121 mg/kg p.o.	T_{max} (h)	C_{max} (μg/ml)	$AUC_{(0-t)}$ (μg•h/ml)	Reference
Prediction	0.24	1.05	0.98	—
Observation 1	0.17 ± 0.00	1.24 ± 0.78	0.79 ± 0.08	Zhang et al. (2011)
Fold error	1.44	1.19	1.25	—
Observation 2	0.17 ± 0.00	1.67 ± 0.85	0.79 ± 0.08	Huang et al. (2014)
Fold error	1.44	1.60	1.25	—

TABLE 10 | Variation span of the experimental *in vitro* parameters and prediction PK parameters in the sensitivity analysis.

	f_u	CL_{int} (μl/min/mg)	T_{max}(h)	C_{max} (μg/ml)	$AUC_{(0-t)}$ (μg•h/ml)
Phenacetin	0.14–0.50	20.70–78.00	0.18–0.28	1.93–15.74	1.10–14.25
Fold range	3.45	3.77	1.56	8.16	12.95
Omeprazole	0.10–0.23	119.00–188.00	0.38–0.46	0.21–0.77	0.26–0.98
Fold range	2.21	1.58	1.21	3.67	3.77
Nifedipine	0.01–0.08	35.18–402	0.36–1.20	0.51–7.40	0.52–47.27
Fold range	8.00	11.43	3.33	14.51	90.90
Chlorzoxazone	0.05–0.373	5.00–38.80	0.29–0.70	37.69–199.27	34.69–1970.18
Fold range	8.11	7.76	2.41	5.29	56.79
Metoprolol	0.80–0.92	17.10–59.90	0.54–0.79	0.15–0.28	0.25–1.02
Fold range	1.16	3.50	1.46	1.87	4.08
Baicalein	0.03–0.08	338.90–574.11	0.19–0.36	0.59–2.08	0.51–2.36
Fold range	2.73	1.69	1.89	3.53	4.63
Tolbutamide	0.02–0.27	2.72–8.10	0.32–0.71	152.72–260.15	231.67–4587.60
Fold range	13.33	2.98	2.22	1.70	19.80

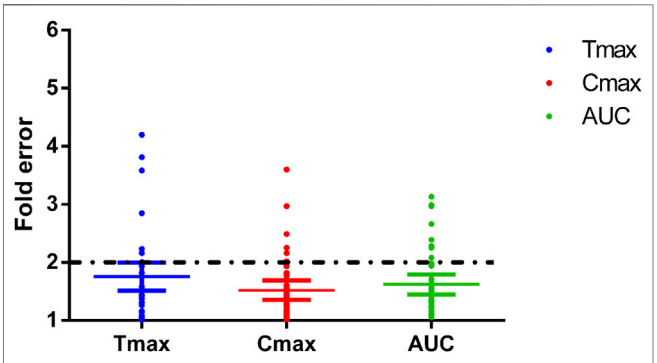

FIGURE 8 | Fold errors of the PK parameters from the PBPK models of phenacetin, tolbutamide, omeprazole, metoprolol, chlorzoxazone, nifedipine, and baicalein. The three lines in each parameter represent mean with 95% confidence interval and the black dotted line across the fold error = 2 represent evaluation criteria.

noting that there is a potential correlation between f_u and CL_{int} under physiological conditions, which likewise may unnaturally increase the variability in predicted values. Furthermore, since the effect of f_u on CL_{int} might be poorly investigated and difficult to obtain from previous studies, the impact of such correlation on the variability of predicted values remains to be further explored.

In the sensitivity analysis, we summarized the variation span of the experimental *in vitro* parameters and prediction PK parameters in **Table 10**. Except for nifedipine (fold error of the observed T_{max} was 3.3), the variation of prediction T_{max} in the sensitivity analysis of other drugs was slight, meaning that the experimental difference of f_u and CL_{int} had little impact on T_{max} compared with C_{max} and $AUC_{(0-t)}$. Compared with phenacetin, omeprazole, metoprolol, and baicalein, the experimental variation of f_u or CL_{int} of nifedipine, chlorzoxazone, and tolbutamide is relatively large (fold errors of f_u or CL_{int} > 8), which led to a large variation span in the sensitivity analysis with the fold errors of C_{max} or $AUC_{(0-t)}$ more than 10. Meanwhile, the variation of both f_u and CL_{int} was higher than 3, resulting in significant fold errors of C_{max} and $AUC_{(0-t)}$ (>8.0). Moreover, inflection points were noted in the change trend graph of f_u and CL_{int} of phenacetin, nifedipine, chlorzoxazone, and tolbutamide shown in the figure of sensitivity analysis, with the prediction value significantly fluctuating around. Therefore, sensitivity analysis is necessary for model construction. That is to say, when the *in vitro* parameters are close to the inflection point, extra attention should be paid to the PBPK model construction.

In addition to using the PSA and HBD methods to predict the absorption of model drugs in the PBPK model, we also explored the prediction accuracy of the PBPK model using P_{app} from *in vitro* experiments such as Caco-2 experimentation. Interestingly, the results showed that the overall prediction performance of PBPK models using the PSA and HBD methods was better. It could be related to defects in the *in vitro* absorption experiments, such as the inability to simulate the dynamic flow of fluids in the body, the lack of mucus layer, the more minor tight junctions, and the thicker unstirred water layer. These may cause the P_{app} to not to truly simulate the diffusion of drugs *in vivo* and thus cannot truly predict the drug absorption degree in the body.

It is worth mentioning that the PBPK model using *in vitro* parameters is beneficial to drug development, and the more accurate the value of *in vitro* parameters, the better fit the model.

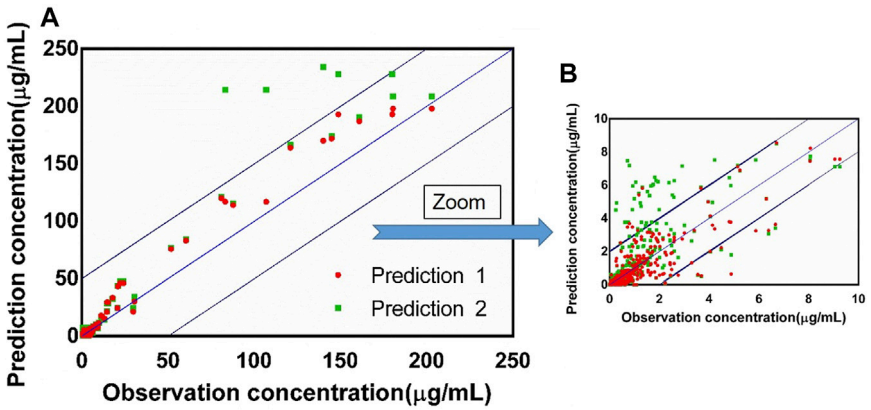

FIGURE 9 | (A) Observed concentration vs. predicted concentration (n = 390) based on the PBPK model with the absorption module using the PSA and HBD models (prediction 1) and the PBPK model using P_{app} from Caco-2 experimentation (prediction 2), blue box: ±20% of the observation concentration; **(B)** graph zoomed at 0–10 μg/ml.

TABLE 11 | Performance of the PBPK model with absorption module using PSA and HBD (prediction 1) and PBPK model using P_{app} from Caco-2 experimentation (prediction 2).

Performance	R^2	MAE	RMSE
Prediction 1	0.82	3.30	10.64
Prediction 2	0.58	4.99	16.01

However, the model compounds we applied were BCS (biopharmaceutics classification system) class II drugs, exhibited linear absorption and primarily cleared *via* metabolism. Therefore, our models were appropriate to the PK prediction of chemicals not affected by transporters such as P-gp (p-glycoprotein) efflux transporter. For other compounds with complex drug metabolism characteristics, using *in vitro* parameters alone to construct a PBPK model and the prediction accuracy still require further research and validation. Moreover, in recent years, with the development of computer technology and *in vitro* experiments, the contribution of PBPK models to advancing 3Rs in new drug development is undoubtedly a hot topic of discussion. Since rodents were widely used in preclinical pharmacological experiments, this study used rats as the model animal when constructing PBPK models based on *in vitro* parameters. It is expected that animal experiments can be reduced in the early stage of drug development with the validation of the feasibility and reliability of the models. However, due to the differences in physiological parameters of other species, the construction of their PBPK models needs further exploration and optimization, and due to the complexity of the human body, whether this method can be directly applied to predict the pharmacokinetic characteristics of candidate compounds in the humans and the reliability of the predicted results still need further exploration.

5 CONCLUSION

In our study, bottom–up PBPK models constructed with *in vitro* data were developed, and popular probe substrates were used as model drugs. Most of the fold errors between the observed PK data with the predicted ones were within the threshold of 2, indicating good prediction accuracy. The influence of *in vitro* data was comprehensively analyzed, and results supported that the model accuracy is related to the precision of the *in vitro* data. Moreover, most of the observed PK data is within the uncertainty range, and R^2 is more than 0.8, indicating the applicability of the PBPK model in the absence of *in vivo* data in the early drug development. In conclusion, a strategy of the bottom–up PBPK model with the quantity of an uncertainty range is constructed, which helps reduce animal experiments and is a good practice of 3Rs in the early screening of candidate compounds.

DATA AVAILABILITY STATEMENT

The original contributions presented in the study are included in the article/**Supplementary Material**, further inquiries can be directed to the corresponding authors.

AUTHOR CONTRIBUTIONS

XX and WC are responsible for this manuscript.

FUNDING

This work was supported by the Shanghai Science and Technology Innovation Fund (18140900900). Certara UK (Simcyp Division) granted free access to the Simcyp® Simulators through an academic license.

SUPPLEMENTARY MATERIAL

The Supplementary Material for this article can be found online at: https://www.frontiersin.org/articles/10.3389/fphar.2022.895556/full#supplementary-material

REFERENCES

Ahn, C. Y., Bae, S. K., Jung, Y. S., Lee, I., Kim, Y. C., Lee, M. G., et al. (2008). Pharmacokinetic Parameters of Chlorzoxazone and its Main Metabolite, 6-hydroxychlorzoxazone, after Intravenous and Oral Administration of Chlorzoxazone to Liver Cirrhotic Rats with Diabetes Mellitus. *Drug Metab. Dispos* 36 (7), 1233–1241. doi:10.1124/dmd.107.017442

Andersen, M. E., Clewell, H. J., 3rd, Gargas, M. L., Smith, F. A., and Reitz, R. H. (1987). Physiologically Based Pharmacokinetics and the Risk Assessment Process for Methylene Chloride. *Toxicol. Appl. Pharmacol.* 87 (2), 185–205. doi:10.1016/0041-008x(87)90281-x

Baek, H. W., Bae, S. K., Lee, M. G., and Sohn, Y. T. (2006). Pharmacokinetics of Chlorzoxazone in Rats with Diabetes: Induction of CYP2E1 on 6-hydroxychlorzoxazone Formation. *J. Pharm. Sci.* 95 (11), 2452–2462. doi:10.1002/jps.20698

Ball, K., Bouzom, F., Scherrmann, J. M., Walther, B., and Declèves, X. (2014). Comparing Translational Population-PBPK Modelling of Brain Microdialysis with Bottom-Up Prediction of Brain-To-Plasma Distribution in Rat and Human. *Biopharm. Drug Dispos* 35 (8), 485–499. doi:10.1002/bdd.1908

Belpaire, F. M., De Smet, F., Chindavijak, B., Fraeyman, N., and Bogaert, M. G. (1989). Effect of Turpentine-Induced Inflammation on the Disposition Kinetics of Propranolol, Metoprolol, and Antipyrine in the Rat. *Fundam. Clin. Pharmacol.* 3 (2), 79–88. doi:10.1111/j.1472-8206.1989.tb00667.x

Belpaire, F. M., de Smet, F., Vynckier, L. J., Vermeulen, A. M., Rosseel, M. T., Bogaert, M. G., et al. (1990). Effect of Aging on the Pharmcokinetics of Atenolol, Metoprolol and Propranolol in the Rat. *J. Pharmacol. Exp. Ther.* 254 (1), 116–122.

Berezhkovskiy, L. M. (2004). Volume of Distribution at Steady State for a Linear Pharmacokinetic System with Peripheral Elimination. *J. Pharm. Sci.* 93 (6), 1628–1640. doi:10.1002/jps.20073

Cao, X., Gibbs, S. T., Fang, L., Miller, H. A., Landowski, C. P., Shin, H. C., et al. (2006). Why Is it Challenging to Predict Intestinal Drug Absorption and Oral Bioavailability in Human Using Rat Model. *Pharm. Res.* 23 (8), 1675–1686. doi:10.1007/s11095-006-9041-2

Cascone, S., Lamberti, G., Marra, F., Titomanlio, G., d'Amore, M., and Barba, A. A. (2016). Gastrointestinal Behavior and ADME Phenomena: I. *In Vitro* Simulation. *J. Drug Deliv. Sci. Techn.* 35, 272–283. doi:10.1016/j.jddst.2016.08.002

Chang, H. Y., Wu, S., Meno-Tetang, G., and Shah, D. K. (2019). A Translational Platform PBPK Model for Antibody Disposition in the Brain. *J. Pharmacokinet. Pharmacodyn* 46 (4), 319–338. doi:10.1007/s10928-019-09641-8

Chen, Y., Jin, J. Y., Mukadam, S., Malhi, V., and Kenny, J. R. (2012). Application of IVIVE and PBPK Modeling in Prospective Prediction of Clinical Pharmacokinetics: Strategy and Approach during the Drug Discovery Phase with Four Case Studies. *Biopharm. Drug Dispos* 33 (2), 85–98. doi:10.1002/bdd.1769

Cheng, W., and Ng, C. A. (2017). A Permeability-Limited Physiologically Based Pharmacokinetic (PBPK) Model for Perfluorooctanoic Acid (PFOA) in Male Rats. *Environ. Sci. Technol.* 51 (17), 9930–9939. doi:10.1021/acs.est.7b02602

Choi, Y. H., and Lee, M. G. (2012). Pharmacokinetic and Pharmacodynamic Interaction between Nifedipine and Metformin in Rats: Competitive Inhibition for Metabolism of Nifedipine and Metformin by Each Other via CYP Isozymes. *Xenobiotica* 42 (5), 483–495. doi:10.3109/00498254.2011.633177

Clewell, R. A., and Clewell, H. J. (2008). Development and Specification of Physiologically Based Pharmacokinetic Models for Use in Risk Assessment. *Regul. Toxicol. Pharmacol.* 50 (1), 129–143. doi:10.1016/j.yrtph.2007.10.012

Dargó, G., Vincze, A., Müller, J., Kiss, H. J., Nagy, Z. Z., and Balogh, G. T. (2019). Corneal-PAMPA: A Novel, Non-cell-based Assay for Prediction of Corneal Drug Permeability. *Eur. J. Pharm. Sci.* 128, 232–239. doi:10.1016/j.ejps.2018.12.012

De Buck, S. S., Sinha, V. K., Fenu, L. A., Nijsen, M. J., Mackie, C. E., and Gilissen, R. A. (2007). Prediction of Human Pharmacokinetics Using Physiologically Based Modeling: A Retrospective Analysis of 26 Clinically Tested Drugs. *Drug Metab. Dispos* 35 (10), 1766–1780. doi:10.1124/dmd.107.015644

Ekins, S., Waller, C. L., Swaan, P. W., Cruciani, G., Wrighton, S. A., and Wikel, J. H. (2000). Progress in Predicting Human ADME Parameters In Silico. *J. Pharmacol. Toxicol. Methods* 44 (1), 251–272. doi:10.1016/s1056-8719(00)00109-x

Ellison, C. A. (2018). Structural and Functional Pharmacokinetic Analogs for Physiologically Based Pharmacokinetic (PBPK) Model Evaluation. *Regul. Toxicol. Pharmacol.* 99, 61–77. doi:10.1016/j.yrtph.2018.09.008

Grundy, J. S., Eliot, L. A., and Foster, R. T. (1997). Extrahepatic First-Pass Metabolism of Nifedipine in the Rat. *Biopharmaceutics & drug disposition* 18 (6), 509–522. doi:10.1002/(sici)1099-081x(199708)18:6<509::aid-bdd38>3.0.co;2-5

Grundy, J. S., Eliot, L. A., Kulmatycki, K. M., and Foster, R. T. (1998). Grapefruit Juice and orange Juice Effects on the Bioavailability of Nifedipine in the Rat. *Biopharmaceutics & drug disposition* 19 (3), 175–183. doi:10.1002/(sici)1099-081x(199804)19:3<175::aid-bdd85>3.0.co;2-7

Haddad, S., Béliveau, M., Tardif, R., and Krishnan, K. (2001). A PBPK Modeling-Based Approach to Account for Interactions in the Health Risk Assessment of Chemical Mixtures. *Toxicol. Sci.* 63 (1), 125–131. doi:10.1093/toxsci/63.1.125

Hariparsad, N., Sane, R. S., Strom, S. C., and Desai, P. B. (2006). *In Vitro* methods in Human Drug Biotransformation Research: Implications for Cancer Chemotherapy. *Toxicol. Vitro* 20 (2), 135–153. doi:10.1016/j.tiv.2005.06.049

Harrison, L. I., and Gibaldi, M. (1977). Physiologically Based Pharmacokinetic Model for Digoxin Disposition in Dogs and its Preliminary Application to Humans. *J. Pharm. Sci.* 66 (12), 1679–1683. doi:10.1002/jps.2600661206

He, J. X., Ohno, K., Tang, J., Hattori, M., Tani, T., and Akao, T. (2014). Da-Chaihu-Tang Alters the Pharmacokinetics of Nifedipine in Rats and a Treatment Regimen to Avoid This. *J. Pharm. Pharmacol.* 66 (11), 1623–1630. doi:10.1111/jphp.12285

Huang, S. M., Abernethy, D. R., Wang, Y., Zhao, P., and Zineh, I. (2013). The Utility of Modeling and Simulation in Drug Development and Regulatory Review. *J. Pharm. Sci.* 102 (9), 2912–2923. doi:10.1002/jps.23570

Huang, Y., Zhang, B., Gao, Y., Zhang, J., and Shi, L. (2014). Baicalein-nicotinamide Cocrystal with Enhanced Solubility, Dissolution, and Oral Bioavailability. *J. Pharm. Sci.* 103 (8), 2330–2337. doi:10.1002/jps.24048

Igari, Y., Sugiyama, Y., Sawada, Y., Iga, T., and Hanano, M. (1983). Prediction of Diazepam Disposition in the Rat and Man by a Physiologically Based Pharmacokinetic Model. *J. Pharmacokinet. biopharmaceutics* 11 (6), 577–593. doi:10.1007/BF01059058

Ikehata, M., Ohnishi, N., Matsumoto, T., Kiyohara, Y., Maeda, A., Kawakita, T., et al. (2008). Effects of Sairei-To on the Pharmacokinetics of Nifedipine in Rats. *Phytother Res.* 22 (1), 12–17. doi:10.1002/ptr.2234

Irvine, J. D., Takahashi, L., Lockhart, K., Cheong, J., Tolan, J. W., Selick, H. E., et al. (1999). MDCK (Madin-Darby Canine Kidney) Cells: A Tool for Membrane Permeability Screening. *J. Pharm. Sci.* 88 (1), 28–33. doi:10.1021/js9803205

Iwao, T., Inoue, K., Hayashi, Y., Yuasa, H., and Watanabe, J. (2002). Metabolic Extraction of Nifedipine during Absorption from the Rat Small Intestine. *Drug Metab. Pharmacokinet.* 17 (6), 546–553. doi:10.2133/dmpk.17.546

Iwatsubo, T., Hirota, N., Ooie, T., Suzuki, H., Shimada, N., Chiba, K., et al. (1997). Prediction of *In Vivo* Drug Metabolism in the Human Liver from *In Vitro* Metabolism Data. *Pharmacol. Ther.* 73 (2), 147–171. doi:10.1016/s0163-7258(96)00184-2

Jia, H., Li, W., and Zhao, K. (2006). Determination of Omeprazole in Rat Plasma by High-Performance Liquid Chromatography without Solvent Extraction. *J. Chromatogr. B Analyt Technol. Biomed. Life Sci.* 837 (1-2), 112–115. doi:10.1016/j.jchromb.2006.04.007

Jin, Z., He, Q., Zhu, X., Zhu, M., Wang, Y., Wu, X. A., et al. (2022). Application of Physiologically Based Pharmacokinetic Modelling for the Prediction of Drug-Drug Interactions Involving Anlotinib as a Perpetrator of Cytochrome P450 Enzymes. *Basic Clin. Pharmacol. Toxicol.* 130, 592. doi:10.1111/bcpt.13721

Kahn, G. C., Rubenfield, M., Davies, D. S., and Boobis, A. R. (1987). Phenacetin O-Deethylase Activity of the Rat: Strain Differences and the Effects of Enzyme-Inducing Compounds. *Xenobiotica* 17 (2), 179–187. doi:10.3109/00498258709043927

Kazuhide, W., Katsushi, F., Kohei, E., Ryozo, O., and Yutaka, G. (1994). First-Pass Metabolism of Omeprazole in Rats. *J. Pharm. Sci.* 83 (8), 1131. doi:10.1002/jps.2600830812

Kim, Y. I., Fluckiger, L., Hoffman, M., Lartaud-Idjouadiene, I., Atkinson, J., and Maincent, P. (1997). The Antihypertensive Effect of Orally Administered Nifedipine-Loaded Nanoparticles in Spontaneously Hypertensive Rats. *Br. J. Pharmacol.* 120 (3), 399–404. doi:10.1038/sj.bjp.0700910

Komura, H., and Iwaki, M. (2005). Pharmacokinetics and Metabolism of Metoprolol and Propranolol in the Female DA and Female Wistar Rat: the Female DA Rat Is Not Always an Animal Model for Poor Metabolizers of CYP2D6. *J. Pharm. Sci.* 94 (2), 397–408. doi:10.1002/jps.20255

Kostewicz, E. S., Aarons, L., Bergstrand, M., Bolger, M. B., Galetin, A., Hatley, O., et al. (2014). PBPK Models for the Prediction of *In Vivo* Performance of Oral Dosage Forms. *Eur. J. Pharm. Sci.* 57, 300–321. doi:10.1016/j.ejps.2013.09.008

Lee, D. Y., Kim, J. W., and Lee, M. G. (2007c). Pharmacokinetic Interaction between Oltipraz and Omeprazole in Rats: Competitive Inhibition of Metabolism of Oltipraz by Omeprazole via CYP1A1 and 3A2, and of Omeprazole by Oltipraz via CYP1A1/2, 2D1/2, and 3A1/2. *Eur. J. Pharm. Sci.* 32 (4-5), 328–339. doi:10.1016/j.ejps.2007.08.008

Lee, D. Y., Jung, Y. S., Kim, Y. C., Kim, S. Y., and Lee, M. G. (2009). Faster Clearance of Omeprazole in Mutant Nagase Analbuminemic Rats: Possible Roles of Increased Protein Expression of Hepatic CYP1A2 and Lower Plasma Protein Binding. *Biopharm. Drug Dispos* 30 (3), 107–116. doi:10.1002/bdd.651

Lee, D. Y., Lee, I., and Lee, M. G. (2007a). Effects of Cysteine on the Pharmacokinetic Parameters of Omeprazole in Rats with Protein-Calorie Malnutrition: Partial Restoration of Some Parameters to Control Levels by Oral Cysteine Supplementation. *J. Parenter. Enteral Nutr.* 31 (1), 37–46. doi:10.1177/014860710703100137

Lee, D. Y., Lee, I., and Lee, M. G. (2007b). Pharmacokinetics of Omeprazole after Intravenous and Oral Administration to Rats with Liver Cirrhosis Induced by Dimethylnitrosamine. *Int. J. Pharm.* 330 (1-2), 37–44. doi:10.1016/j.ijpharm.2006.08.037

Lee, D. Y., Shin, H. S., Lee, I., and Lee, M. G. (2006). Pharmacokinetics of Omeprazole in Rats with Water Deprivation for 72 hours. *Biopharm. Drug Dispos* 27 (8), 361–370. doi:10.1002/bdd.516

Li, S., Yu, Y., Bian, X., Yao, L., Li, M., Lou, Y. R., et al. (2021). Prediction of Oral Hepatotoxic Dose of Natural Products Derived from Traditional Chinese Medicines Based on SVM Classifier and PBPK Modeling. *Arch. Toxicol.* 95 (5), 1683–1701. doi:10.1007/s00204-021-03023-1

Lin, J. H., and Lu, A. Y. (1997). Role of Pharmacokinetics and Metabolism in Drug Discovery and Development. *Pharmacol. Rev.* 49 (4), 403–449.

Lindstrom, F. T., Gillett, J. W., and Rodecap, S. E. (1974). Distribution of HEOD (Dieldrin) in Mammals. I. Preliminary Model. *Arch. Environ. Contam. Toxicol.* 2 (1), 9–42. doi:10.1007/bf01985798

Lombardo, F., Desai, P. V., Arimoto, R., Desino, K. E., Fischer, H., Keefer, C. E., et al. (2017). In Silico Absorption, Distribution, Metabolism, Excretion, and Pharmacokinetics (ADME-PK): Utility and Best Practices. An Industry Perspective from the International Consortium for Innovation through Quality in Pharmaceutical Development. *J. Med. Chem.* 60 (22), 9097–9113. doi:10.1021/acs.jmedchem.7b00487

Ma, J., Wang, S., Zhang, M., Zhang, Q., Zhou, Y., Lin, C., et al. (2015). Simultaneous Determination of Bupropion, Metroprolol, Midazolam, Phenacetin, Omeprazole and Tolbutamide in Rat Plasma by UPLC-MS/MS and its Application to Cytochrome P450 Activity Study in Rats. *Biomed. Chromatogr.* 29 (8), 1203–1212. doi:10.1002/bmc.3409

Meek, M. E., Barton, H. A., Bessems, J. G., Lipscomb, J. C., and Krishnan, K. (2013). Case Study Illustrating the WHO IPCS Guidance on Characterization and Application of Physiologically Based Pharmacokinetic Models in Risk Assessment. *Regul. Toxicol. Pharmacol.* 66 (1), 116–129. doi:10.1016/j.yrtph.2013.03.005

Mielke, H., and Gundert-Remy, U. (2009). Bisphenol A Levels in Blood Depend on Age and Exposure. *Toxicol. Lett.* 190 (1), 32–40. doi:10.1016/j.toxlet.2009.06.861

Mielke, H., Partosch, F., and Gundert-Remy, U. (2011). The Contribution of Dermal Exposure to the Internal Exposure of Bisphenol A in Man. *Toxicol. Lett.* 204 (2-3), 190–198. doi:10.1016/j.toxlet.2011.04.032

Miller, N. A., Reddy, M. B., Heikkinen, A. T., Lukacova, V., and Parrott, N. (2019). Physiologically Based Pharmacokinetic Modelling for First-In-Human Predictions: An Updated Model Building Strategy Illustrated with Challenging Industry Case Studies. *Clin. Pharmacokinet.* 58 (6), 727–746. doi:10.1007/s40262-019-00741-9

Mutsunobu, Y., Noriaki, O., Noriko, S., Suguru, E., Koji, T., Teruyoshi, Y., et al. (2004). Studies on Interactions between Functional Foods or Dietary Supplements and Medicines. III. Effects of Ginkgo Biloba Leaf Extract on the Pharmacokinetics of Nifedipine in Rats. *Biol. Pharm. Bull.* 27 (12), 1315–1320. doi:10.1248/bpb.26.1315

Nandi, U., Dan, S., and Pal, T. K. (2015). Development and Validation of a Liquid Chromatography–Mass Spectrometry Method for Simultaneous Determination of Metoprolol and Telmisartan in Rat Plasma and its Application to Pharmacokinetic Study. *J. Pharm. Invest.* 45 (3), 329–340. doi:10.1007/s40005-015-0180-5

Nandi, U., Karmakar, S., Das, A. K., Ghosh, B., Padman, A., Chatterjee, N., et al. (2013). Pharmacokinetics, Pharmacodynamics and Toxicity of a Combination of Metoprolol Succinate and Telmisartan in Wistar Albino Rats: Safety Profiling. *Regul. Toxicol. Pharmacol.* 65 (1), 68–78. doi:10.1016/j.yrtph.2012.11.001

Nestorov, I. (2003). Whole Body Pharmacokinetic Models. *Clin. Pharmacokinet.* 42 (10), 883–908. doi:10.2165/00003088-200342100-00002

Nishimura, N., Naora, K., Hirano, H., and Iwamoto, K. (1999). A Chinese Traditional Medicine, Sho-Saiko-To (Xiao-chaihu-tang), Reduces the Bioavailability of Tolbutamide after Oral Administration in Rats. *Am. J. Chin. Med.* 27 (3-4), 355–363. doi:10.1142/S0192415X99000409

Nishimura, N., Naora, K., Hirano, H., and Iwamoto, K. (1998). Effects of Sho-Saiko-To on the Pharmacokinetics and Pharmacodynamics of Tolbutamide in Rats. *J. Pharm. Pharmacol.* 50 (2), 231–236. doi:10.1111/j.2042-7158.1998.tb06181.x

Paini, A., Leonard, J. A., Joossens, E., Bessems, J. G. M., Desalegn, A., Dorne, J. L., et al. (2019). Next Generation Physiologically Based Kinetic (NG-PBK) Models in Support of Regulatory Decision Making. *Comput. Toxicol.* 9, 61–72. doi:10.1016/j.comtox.2018.11.002

Pang, K. S., and Rowland, M. (1977). Hepatic Clearance of Drugs. I. Theoretical Considerations of a "Well-Stirred" Model and a "parallel Tube" Model. Influence of Hepatic Blood Flow, Plasma and Blood Cell Binding, and the Hepatocellular Enzymatic Activity on Hepatic Drug Clearance. *J. Pharmacokinet. Biopharm.* 5 (6), 625–653. doi:10.1007/bf01059688

Paul, N. M. (1991). Omeprazole. *N. Engl. J. Med.* 324, 965–975. doi:10.1056/NEJM199104043241406

Pelkonen, O., and Turpeinen, M. (2007). In Vitro-In Vivo Extrapolation of Hepatic Clearance: Biological Tools, Scaling Factors, Model Assumptions and Correct Concentrations. *Xenobiotica* 37 (10-11), 1066–1089. doi:10.1080/00498250701620726

Pi, J., Wang, S., Li, W., Kebebe, D., Zhang, Y., Zhang, B., et al. (2019). A Nano-Cocrystal Strategy to Improve the Dissolution Rate and Oral Bioavailability of Baicalein. *Asian J. Pharm. Sci.* 14 (2), 154–164. doi:10.1016/j.ajps.2018.04.009

Poulin, P., and Theil, F. P. (2002). Prediction of Pharmacokinetics Prior to *In Vivo* Studies. 1. Mechanism-Based Prediction of Volume of Distribution. *J. Pharm. Sci.* 91 (1), 129–156. doi:10.1002/jps.10005

Prentis, R. A., Lis, Y., and Walker, S. R. (1988). Pharmaceutical Innovation by the Seven UK-owned Pharmaceutical Companies (1964-1985). *Br. J. Clin. Pharmacol.* 25 (3), 387–396. doi:10.1111/j.1365-2125.1988.tb03318.x

Raunio, H., Taavitsainen, P., Honkakoski, P., Juvonen, R., and Pelkonen, O. (2004). *In Vitro* methods in the Prediction of Kinetics of Drugs: Focus on Drug Metabolism. *Altern. Lab. Anim.* 32 (4), 425–430. doi:10.1177/026119290403200415

Regårdh, C. G., Gabrielsson, M., Hoffman, K. J., Löfberg, I., and Skånberg, I. (1985). Pharmacokinetics and Metabolism of Omeprazole in Animals and Man - an Overview. *Scand. J. Gastroenterol.* 20 (Suppl. 108), 79–94. doi:10.3109/00365528509095821

Rietjens, I. M. C. M., Punt, A., Schilter, B., Scholz, G., Delatour, T., and van Bladeren, P. J. (2010). In Silico methods for Physiologically Based Biokinetic Models Describing Bioactivation and Detoxification of Coumarin and Estragole: Implications for Risk Assessment. *Mol. Nutr. Food Res.* 54 (2), 195–207. doi:10.1002/mnfr.200900211

Rodgers, T., Leahy, D., and Rowland, M. (2005). Tissue Distribution of Basic Drugs: Accounting for Enantiomeric, Compound and Regional Differences Amongst Beta-Blocking Drugs in Rat. *J. Pharm. Sci.* 94 (6), 1237–1248. doi:10.1002/jps.20323

Rodgers, T., and Rowland, M. (2007). Mechanistic Approaches to Volume of Distribution Predictions: Understanding the Processes. *Pharm. Res.* 24 (5), 918–933. doi:10.1007/s11095-006-9210-3

Rostami-Hodjegan, A., and Tucker, G. T. (2007). Simulation and Prediction of *In Vivo* Drug Metabolism in Human Populations from *In Vitro* Data. *Nat. Rev. Drug Discov.* 6 (2), 140–148. doi:10.1038/nrd2173

Rowland, M., Peck, C., and Tucker, G. (2011). Physiologically-based Pharmacokinetics in Drug Development and Regulatory Science. *Annu. Rev. Pharmacol. Toxicol.* 51, 45–73. doi:10.1146/annurev-pharmtox-010510-100540

Singh, D., and Asad, M. (2010). Effect of Soybean Administration on the Pharmacokinetics of Carbamazepine and Omeprazole in Rats. *Fundam. Clin. Pharmacol.* 24 (3), 351–355. doi:10.1111/j.1472-8206.2009.00762.x

Sun, D., Lennernas, H., Welage, L. S., Barnett, J. L., Landowski, C. P., Foster, D., et al. (2002). Comparison of Human Duodenum and Caco-2 Gene Expression Profiles for 12,000 Gene Sequences Tags and Correlation with Permeability of 26 Drugs. *Pharm. Res.* 19 (10), 1400–1416. doi:10.1023/a:1020483911355

Sun, W., Wang, Z., Chen, R., Huang, C., Sun, R., Hu, X., et al. (2017). Influences of Anlotinib on Cytochrome P450 Enzymes in Rats Using a Cocktail Method. *Biomed. Res. Int.* 2017, 3619723. doi:10.1155/2017/3619723

Taylor, K., and Alvarez, L. R. (2019). An Estimate of the Number of Animals Used for Scientific Purposes Worldwide in 2015. *Altern. Lab. Anim.* 47 (5-6), 196–213. doi:10.1177/0261192919899853

Tchaparian, E., Xu, G., Huang, T., and Jin, L. (2008). "Cell Based Experimental Models as Tools for the Prediction of Human Intestinal Absorption," in Poster Presentation, 15th North American Regional International Society for the Study of Xenobiotics Meeting.

Templeton, I. E., Jones, N. S., and Musib, L. (2018). Pediatric Dose Selection and Utility of PBPK in Determining Dose. *Aaps j* 20 (2), 31. doi:10.1208/s12248-018-0187-8

T'jollyn, H., Vermeulen, A., and Van Bocxlaer, J. (2018). PBPK and its Virtual Populations: the Impact of Physiology on Pediatric Pharmacokinetic Predictions of Tramadol. *AAPS J.* 21 (1), 8. doi:10.1208/s12248-018-0277-7

Umehara, K., Huth, F., Jin, Y., Schiller, H., Aslanis, V., Heimbach, T., et al. (2019). Drug-drug Interaction (DDI) Assessments of Ruxolitinib, a Dual Substrate of CYP3A4 and CYP2C9, Using a Verified Physiologically Based Pharmacokinetic (PBPK) Model to Support Regulatory Submissions. *Drug Metab. Pers Ther.* 34 (2). doi:10.1515/dmpt-2018-0042

van de Kerkhof, E. G., de Graaf, I. A., and Groothuis, G. M. (2007). *In Vitro* methods to Study Intestinal Drug Metabolism. *Curr. Drug Metab.* 8 (7), 658–675. doi:10.2174/138920007782109742

Verhoeckx, K., Cotter, P., López-Expósito, I., Kleiveland, C., Lea, T., Mackie, A., et al. (2015). *The Impact of Food Bioactives on Health:* In Vitro *and* Ex Vivo *Models*. Cham (CH): Springer. doi:10.1007/978-3-319-16104-4_10

Vitale, A., Manciocco, A., and Alleva, E. (2009). The 3R Principle and the Use of Non-human Primates in the Study of Neurodegenerative Diseases: the Case of Parkinson's Disease. *Neurosci. Biobehav Rev.* 33 (1), 33–47. doi:10.1016/j.neubiorev.2008.08.006

Wachsmuth, L., Mensen, A., Barca, C., Wiart, M., Tristão-Pereira, C., Busato, A., et al. (2021). Contribution of Preclinical MRI to Responsible Animal Research: Living up to the 3R Principle. *Magn. Reson. Mater. Phys. Biol. Med.* 34 (4), 469–474. doi:10.1007/s10334-021-00929-w

Wagner, J. G. (1981). History of Pharmacokinetics. *Pharmacol. Ther.* 12 (3), 537–562. doi:10.1016/0163-7258(81)90097-8

Wang, X., Chen, M., Chen, X., Ma, J., Wen, C., Pan, J., et al. (2014). The Effects of Acute Hydrogen Sulfide Poisoning on Cytochrome P450 Isoforms Activity in Rats. *Biomed. Res. Int.* 2014, 209393. doi:10.1155/2014/209393

Wang, Y., Zou, M. J., Zhao, N., Ren, J. G., Zhou, H., and Cheng, G. (2011). Effect of Diallyl Trisulfide on the Pharmacokinetics of Nifedipine in Rats. *J. Food Sci.* 76 (1), T30–T34. doi:10.1111/j.1750-3841.2010.01960.x

Watanabe, K., Matsuka, N., Okazaki, M., Hashimoto, Y., Araki, H., and Gomita, Y. (2002). The Effect of Immobilization Stress on the Pharmacokinetics of Omeprazole in Rats. *Acta Med. Okayama* 56 (1), 19–23. doi:10.14712/18059694.2019.52

Welch, R. M., Hughes, C. R., and Deangelis, R. L. (1976). Effect of 3-methylcholanthrene Pretreatment on the Bioavailability of Phenacetin in the Rat. *Drug Metab. disposition: Biol. fate chemicals* 4 (4), 402–406.

Winiwarter, S., Bonham, N. M., Ax, F., Hallberg, A., Lennernäs, H., and Karlén, A. (1998). Correlation of Human Jejunal Permeability (*In Vivo*) of Drugs with Experimentally and Theoretically Derived Parameters. A Multivariate Data Analysis Approach. *J. Med. Chem.* 41 (25), 4939–4949. doi:10.1021/jm9810102

Yamashita, F., and Hashida, M. (2004). In Silico approaches for Predicting ADME Properties of Drugs. *Drug Metab. Pharmacokinet.* 19 (5), 327–338. doi:10.2133/dmpk.19.327

Yamazaki, S., Skaptason, J., Romero, D., Vekich, S., Jones, H. M., Tan, W., et al. (2011). Prediction of Oral Pharmacokinetics of cMet Kinase Inhibitors in Humans: Physiologically Based Pharmacokinetic Model versus Traditional One-Compartment Model. *Drug Metab. Disposition* 39 (3), 383. doi:10.1124/dmd.110.035857

Yoon, I. S., Choi, M. K., Kim, J. S., Shim, C. K., Chung, S. J., and Kim, D. D. (2011). Pharmacokinetics and First-Pass Elimination of Metoprolol in Rats: Contribution of Intestinal First-Pass Extraction to Low Bioavailability of Metoprolol. *Xenobiotica* 41 (3), 243–251. doi:10.3109/00498254.2010.538090

Young, L. D., Lee, MG, Sook, S. H., and Inchul, L. (2007). Changes in Omeprazole Pharmacokinetics in Rats with Diabetes Induced by Alloxan or Streptozotocin: Faster Clearance of Omeprazole Due to Induction of Hepatic CYP1A2 and 3A1. *J. Pharm. Pharm. Sci.* 10 (4), 420–433. doi:10.18433/j3wc7g

Zhang, J., Lv, H., Jiang, K., and Gao, Y. (2011). Enhanced Bioavailability after Oral and Pulmonary Administration of Baicalein Nanocrystal. *Int. J. Pharm.* 420 (1), 180–188. doi:10.1016/j.ijpharm.2011.08.023

Zhang, X., Yang, Y., Grimstein, M., Fan, J., Grillo, J. A., Huang, S. M., et al. (2020). Application of PBPK Modeling and Simulation for Regulatory Decision Making and its Impact on US Prescribing Information: An Update on the 2018-2019 Submissions to the US FDA's Office of Clinical Pharmacology. *J. Clin. Pharmacol.* 60 (Suppl. 1), S160–s178. doi:10.1002/jcph.1767

Zhou, Y., Wang, S., Ding, T., Chen, M., Wang, L., Wu, M., et al. (2014). Evaluation of the Effect of Apatinib (YN968D1) on Cytochrome P450 Enzymes with Cocktail Probe Drugs in Rats by UPLC-MS/MS. *J. Chromatogr. B Analyt Technol. Biomed. Life Sci.* 973C, 68–75. doi:10.1016/j.jchromb.2014.10.013

Conflict of Interest: The authors declare that the research was conducted in the absence of any commercial or financial relationships that could be construed as a potential conflict of interest.